Journal of Hydrology 571 (2019) 627–641

Contents lists available at ScienceDirect

Journal of Hydrology

journal homepage: www.elsevier.com/locate/jhydrol

Research papers

# Exploring stochastic climate uncertainty in space and time using a gridded hourly weather generator

Nadav Peleg*, Peter Molnar, Paolo Burlando, Simone Fatichi

*Institute of Environmental Engineering, Hydrology and Water Resources Management, ETH Zurich, Zurich, Switzerland*

ARTICLE INFO

This manuscript was handled by Andras Bardossy, Editor-in-Chief, with the assistance of Uwe Haberlandt, Associate Editor

*Keywords:*
Weather generator
Stochastic downscaling
Climate change
Internal climate variability
Climate uncertainty
High-resolution rainfall model

ABSTRACT

Exploring the effects of climate change on the hydrological response at the local scale requires climate data at high spatial and temporal resolutions. This is best achieved by generating downscaled ensembles of future climate variables derived from climate models. For this purpose we present a methodology to re-parameterize the AWE-GEN-2d model (Advanced WEather GENerator for a two-dimensional grid). The model simulates key meteorological variables needed by hydrological models and is particularly suitable to explore the effects of stochastic (natural) climatic uncertainty, which is fundamental for hydrological applications, especially at sub-kilometer and hourly scales. Factors of change for different climate statistics are calculated from climate model simulations of present and future climates and subsequently applied to the statistics derived from observations to re-parameterize AWE-GEN-2d. The model abilities in generating an ensemble of future climate variables for the transient period 2020–2089 is presented with examples of precipitation and near-surface air temperature fields from hourly to multi-annual scales for a small mountainous region in the Swiss Alps. The stochastic uncertainty is examined for present and future periods and for spatial scales from the RCM scale (12-km, daily) to 2-km demonstrating the potential use of AWE-GEN-2d outputs. At the RCM scale, model results yield a small increase in annual precipitation (4%) which is within the stochastic uncertainty range for present and future periods (7%). At the fine scale of 2-km, the increase in annual precipitation can exceed the stochastic uncertainty, but for less than 10% of the domain area. On the contrary, changes in annual near-surface air temperature exceed stochastic uncertainty both at the RCM and finer scales. Stochastic climate uncertainty was concluded to be very similar when comparing present and future periods and 12-km and 2-km scales. The benefits of using AWE-GEN-2d in hydrological climate change impact assessments are finally discussed.

## 1. Introduction

The effects of climate change on hydrology are important as they might impose changes to the hydrological cycle and water resources at regional and local scales that exceed the historical natural variability (IPCC, 2018). Hydrological models of different complexity are commonly used to explore and quantify these effects. The typical procedure is to feed the hydrological model with climate variable inputs that are derived directly or indirectly from General Circulation Models (GCMs) or Regional Climate Models (RCMs) (Burlando and Rosso, 2002; Christensen et al., 2004; Xu, 1999; Xu et al., 2005). The demand from policymakers to provide more targeted assessments of local climate impacts, generates a need for climate projections at higher spatial and temporal resolution than delivered from GCMs and most RCMs (Kerr, 2011; Fatichi et al., 2016a). Data from GCMs and RCMs are most often downscaled to match the spatial and temporal resolution required by the hydrological model (Fowler et al., 2007; Wilby and Wigley, 1997; Wood et al., 2004) and/or bias-corrected to fit the observations in the region of interest (Ehret et al., 2012; Peleg et al., 2015a; Teutschbein and Seibert, 2012).

There are three general types of downscaling methods: dynamical, statistical, and stochastic (Fowler et al., 2007; Hewitson and Crane, 1996; Maraun et al., 2010; Murphy, 1999). In dynamical downscaling, RCMs are forced with boundary conditions derived from GCMs to solve the physics of the climate system at a finer spatial and temporal resolution than the parent model in a given sub-domain (Giorgi, 1990, 1995; Giorgi and Mearns, 1991). While dynamical downscaling is robust and physically sound, it has a fundamental limitation as it requires massive computational resources, long running times and expertise in setting and running the models (Gutmann et al., 2016; Leutwyler et al., 2016; Prein et al., 2015). This limitation has made this approach historically less appealing for most hydrologists.

* Corresponding author at: Institute of Environmental Engineering, ETH Zurich, HIL D21.1, Stefano-Franscini-Platz 5, 8093 Zurich, Switzerland.
*E-mail address:* nadav.peleg@sccer-soe.ethz.ch (N. Peleg).

https://doi.org/10.1016/j.jhydrol.2019.02.010
Received 7 August 2018; Received in revised form 3 February 2019; Accepted 5 February 2019
Available online 14 February 2019
0022-1694/ © 2019 Elsevier B.V. All rights reserved.

Statistical downscaling methods (Fealy and Sweeney, 2007; Fowler et al., 2000; Katz, 1996; Jakob Themeßl et al., 2011; Wilby and Wigley, 1997), such as linear regression, bias correction and quantile mapping, link GCM or RCM outputs (predictors) directly to local variables of interest (predictants) using some statistical methodology. Contrary to dynamical downscaling, they are parsimonious in terms of computational cost and do not require specific expertise other than common statistical knowledge. Therefore, statistical downscaling methods have been particularly popular for generating climate forcing subsequently used for hydrological climate impacts (e.g. Teutschbein and Seibert, 2012). A variant of statistical downscaling is stochastic downscaling and its general concept is to randomize the relation between predictors and predictants to account for natural climate variability together with the climate change signal.

An important issue in hydrological climate impact studies is the assessment of future uncertainties. The uncertainty in climate is composed of three main sources: emission scenario uncertainty, climate model uncertainty and stochastic uncertainty (also known as internal or natural climate variability) (for further discussion see, e.g. Deser et al., 2012a; Fatichi et al., 2016a; Hawkins and Sutton, 2009). Emission scenario uncertainty reflects the poor knowledge of the future trajectory of greenhouse gas emissions that depends on socio-economic projections (Meinshausen et al., 2011; van Vuuren et al., 2011). Climate model uncertainty is related to the different responses of GCMs or RCMs used to simulate the future climate for a given emission scenario; the uncertainty emerges partially from the numerical approximations and parameterizations schemes used to describe the physical processes involved within the models and largely from the representation of subgrid scale physical processes (Slingo and Palmer, 2011). Stochastic uncertainty originates from the chaotic nature of the climate system (Deser et al. 2012a) and is due to variations that are directly driven by a purely periodic external forcing, variations due to the non-linear interplay of feedbacks within the climate system, and variations associated with random fluctuations in physical or chemical factors in the atmosphere (Ghil, 2002). It is vital to understand how climate uncertainty is partitioned into these sources, and indeed many past studies proposed different approaches to tackle this issue (e.g. Deser et al., 2012a, 2012b; Fatichi et al., 2016a, 2016b; Hawkins and Sutton, 2009, 2011; Hingray and Said, 2014; Olonscheck and Notz, 2017), considering for example the dependency or independency between climate variables, stationary and nonstationary assumptions, various spatial and temporal scales and analyses for average climate or extremes.

The first two sources of climate uncertainty can be quantified when more than one emission scenario and several climate trajectories, derived from different climate models, are available. The climate model uncertainty can also be quantified based on the assumptions, simplifications and limitations of the climate models. Conversely, to compute the stochastic uncertainty, an ensemble composed of multiple realizations representing the same climate model and emission scenario is required. The rationale is that each climate realization in the ensemble is a potential outcome with the same probability as the other realizations, which differ from each other due to the chaotic nature of climate. For example, the future period of 2070–2099 can be represented by an ensemble that is composed of 50 or 100 realizations corresponding to a specific climate change trajectory, each one 30 years long. The stochastic uncertainty for a given climate variable in such a future can be computed with the median value of all ensemble members and a percentile range obtained from the 50 or 100 realizations (e.g. Fatichi et al., 2016a; Hawkins and Sutton, 2011). This operation can be repeated for different climate variables, different levels of temporal aggregation (e.g. hourly, daily), and various statistics (e.g. mean, variance) of a given variable.

The impacts of considering stochastic uncertainty were explored in hydrological studies that estimated future reservoir levels (Fatichi et al., 2015), future streamflow (Addor et al., 2014; Camici et al., 2017; Giuntoli et al., 2018; Peleg et al., 2015b) and urban flows (Peleg et al., 2017a). Generally, the relative contribution of stochastic uncertainty to the total uncertainty increases as finer spatial scales are considered (Fatichi et al., 2016a; Hawkins and Sutton, 2011), e.g. when exploring hydrological climate impacts over medium ($10^2$–$10^3$ km$^2$) to small ($< 10^2$ km$^2$) catchments and when precipitation is the variable of interest. Therefore, it is advisable to generate multiple realizations when downscaling climate variables from GCMs or RCMs. Dynamical downscaling could be used to generate multiple realizations at the catchment scale, but this option is not yet convenient due to the large computational costs. Also statistical downscaling methods, in their basic structure (i.e. with deterministic relations between predictors and predictants), do not allow a direct exploration of the stochastic uncertainty.

Stochastic downscaling is often performed using stochastic models of simple climatic variables, typically precipitation and temperature (e.g. Bordoy and Burlando, 2014; Burlando and Rosso, 1991; Wasko and Sharma, 2017), or using weather generators (WG) (see Fatichi et al., 2011; Fowler et al., 2005, 2007; Kilsby et al., 2007; Peleg et al., 2017b; Semenov and Barrow, 1997; Wilks and Wilby, 1999), which have been widely applied in hydrological studies (e.g. Camici et al., 2017; Caracciolo et al., 2014; Fatichi et al., 2015; Park and Kim, 2014; Paschalis et al., 2014; Peleg and Morin, 2014; Peleg et al., 2015b; Singer and Michaelides, 2017; Singer et al., 2018; Wheater et al., 2005, and many more). WGs simulate time series for a given climate variable for the present climate. In the downscaling approach, statistics for the present climate are modified to reproduce the statistics of a given future climate exploiting the change in statistics between the two periods that are obtained from GCMs or RCMs (e.g. Fatichi et al., 2011, 2013).

Most WGs are designed as single or multi-site tools, simulating the climate variables at a daily resolution (e.g. Hutchinson, 1995; Keller et al., 2015; Park et al., 2018). Climate time series at this resolution are adequate for certain hydrological applications, especially if large catchments are examined and lumped or semi-distributed hydrological models are used (e.g. Teutschbein et al., 2011). However, the increased availability and use of distributed hydrological models in the context of climate change impact analyses (Fatichi et al., 2015, 2016b; Perra et al., 2018) and the importance of addressing the spatial variability of extremes generate a need for climate projections at higher spatial and temporal resolution. The requirement for high space-time resolutions was recently met by a new stochastic WG named AWE-GEN-2d (Peleg et al., 2017b) that simulates key climate variables that are needed as input into hydrological models in a gridded form at resolutions as high as 100 m × 100 m and 10 min. In this manuscript, we introduce a methodology for using AWE-GEN-2d as a tool to downscale future climate variables (e.g. precipitation and near-surface air temperature) by modifying the parameters of AWE-GEN-2d that were calibrated using observed data for the present climate with information derived from RCM simulations. AWE-GEN-2d is intended to satisfy the hydrologists' needs in generating multiple realizations of a given climate at a spatial and temporal resolution that is adequate for hydrological modeling purposes. We discuss the assumptions, advantages, capabilities and limitations of using AWE-GEN-2d as a non-stationary simulator to downscale climate variables for a transient climate period. In addition, we use AWE-GEN-2d to explore the role of stochastic uncertainty at different spatial scales – the RCM scale ($13 \times 13$ km$^2$) and a finer $2 \times 2$ km$^2$ scale. Last, we discuss the importance of using a high resolution gridded stochastic downscaling method when making hydrological predictions at local spatial scales.

AWE-GEN-2d is briefly described in the following section and its re-parameterization scheme is presented thereafter. The re-parameterization, the simulation of a future downscaled ensemble of climate projections and the analysis of the stochastic uncertainty is demonstrated for the Engelberg region, a mountainous area in the Swiss Alps.

**Table 1**
A list of factors of change used for the re-parameterization of AWE-GEN-2d. The parameters follow the notation in Peleg et al. (2017b). Grid cell – factors of change are calculated for each individual grid cell; Domain – factors of change are the same for all grid cells in the domain.

| Statistic | Parameters affected | Temporal aggregation | Spatial scale |
|---|---|---|---|
| Precipitation occurrence | $R_p(x,y)$ | Daily | Grid cell |
| Mean of precipitation intensity | $GP(\kappa_o,\sigma_o,\theta_o)$ | Daily | Grid cell |
| Variance of precipitation intensity | | Daily | Grid cell |
| Mean of cloud cover | $J(\alpha_{car},\beta_{car},\mu_{car},\sigma_{car})$ | Daily | Domain |
| Standard deviation of cloud cover | | Daily | Domain |
| Kurtosis of cloud cover | | Daily | Domain |
| Skewness of cloud cover | | Daily | Domain |
| Mean of near-surface air temperature | $T(x,y,t)$ | Monthly | Domain |

## 2. Methods

### 2.1. AWE-GEN-2d model

AWE-GEN-2d (Advanced WEather GENerator for a 2-dimensional grid) (Peleg et al., 2017b) is a stochastic weather generator that simulates gridded climate variables at high spatial (sub-kilometer) and temporal (sub-daily) resolutions. It is a substantial evolution of the 1-dimensional AWE-GEN model (Fatichi et al., 2011; Ivanov et al., 2007) and was further developed using methods from three preceding models: (i) STREAP (Paschalis et al., 2013); (ii) HiReS-WG (Peleg and Morin, 2014); and (iii) WINDS (Burlando et al., 2007). AWE-GEN-2d simulates key climate variables that are needed for hydrological, ecological and agricultural applications (e.g. precipitation, cloud cover, near-surface air temperature, solar radiation, vapor pressure and relative humidity) using a combination of stochastic and process-based methods. A brief description of how the model simulates key hydrological variables, precipitation, cloud cover and near-surface air temperature, is provided in the following paragraphs. For further details, the reader is referred to Peleg et al. (2017b).

Precipitation fields are simulated in three stages. First, a temporal sequence of dry and wet spells affecting the entire domain is defined using an alternating renewal process (Peleg and Morin, 2014) in which the wet-dry durations are sampled from specific probability distributions and are mutually independent. Second, a Gaussian stochastic process with a covariance function belonging to the Whittle-Matern class (Gneiting et al., 2010) is used for the simulation of the areal statistics of precipitation and cloud cover for each wet period, these are the wet area ratio, the mean areal precipitation intensity and the cloud area ratio. These three variables are auto- and cross-correlated and thus have to be simulated as a tri-variate stochastic process. Third, the time series of wet area ratio and mean areal precipitation intensity are transformed into precipitation intensity fields (Paschalis et al., 2013). For that, two-dimensional intermittent Gaussian fields, correlated in space and time, are simulated using a Fast Fourier Transform (FFT) method (Lang and Potthoff, 2011). The generated precipitation intensity fields are treated as continuous in space between the east-west and south-north boundaries due to the symmetries of the FFT (Paschalis et al., 2013). This property is exploited to simulate advection of the fields. A bi-variate autoregressive model (Schneider and Neumaier, 2001) is used to simulate time series of the advection (speed and direction) velocities along the east-west and south-north components. Two spatial filters are applied to the precipitation fields (Peleg et al., 2017b). The first filter allows precipitation occurrence to be heterogeneous in space, meaning it is used to generate regions in the field where precipitation occurrence is higher or lower than average. The second filter adjust the probability distribution of precipitation intensity for each grid cell based on a Generalized Pareto (GP) distribution, i.e. allowing spatial heterogeneity in precipitation intensity.

During a wet spell, the cloudiness and precipitation intensity fields are assumed to be cross-correlated, meaning that the intermittent Gaussian fields are used for the generation of both precipitation and cloud fields. During a dry spell, mean cloudiness in the domain is simulated through an autoregressive moving average model with a structure that forces the cloudiness to decay as a function of the time passed since the end of the previous wet spell and to increase toward the beginning of the next wet spell (Fatichi et al., 2011). The Johnson distribution (Johnson, 1949) is used to transform the autoregressive moving average model outputs into a time series of cloud area ratio.

Near-surface air temperature is first simulated for a given reference level as the sum of a 1st order autoregressive model with a stochastic term and a deterministic component (Curtis and Eagleson, 1982; Fatichi et al., 2011; Ivanov et al., 2007; Peleg et al., 2017b), and is then spatially distributed using a stochastic lapse rate. The deterministic component is represented by the time derivative of air temperature, which is a function of the air temperature itself, the incoming longwave radiation, which is dependent on cloud cover (Juszak and Pellicciotti, 2013), and the hourly position of the Sun (Eagleson, 2005). Effects of shading in the terrain, i.e. when the surface is shadowed by surrounding terrain, are also accounted for (Chen et al., 2006; Dubayah and Loechel, 1997). Further details about AWE-GEN-2d can be found in the Technical Reference of the model (Peleg et al., 2017b).

### 2.2. Re-parameterizing AWE-GEN-2d for the future climate

AWE-GEN-2d can be used to generate multiple realizations of future climate. The approach to this end consists of re-parameterizing several of the parameters of AWE-GEN-2d (listed in Table 1) that were estimated from observed data. The new parameters are based on modified climate statistics inferred from climate model outputs (GCMs or RCMs) and are considered representative of the future climate. The approach downscales key climate variables that were simulated by climate models at their original spatial and temporal resolutions (i.e. $10^1$–$10^2$ km and daily) to much finer resolution (e.g. $10^0$ km and hourly). As it is often the case for climate downscaling, this approach is based on the unverifiable assumptions that GCMs and RCMs changes in climate statistics are robust signals of climate change and that the weather generator structure is transferring those changes into finer resolutions accurately.

The “factors of change” (FC) approach (Anandhi et al., 2011; Bordoy and Burlando, 2014; Burlando and Rosso, 1991; Fatichi et al., 2011; Kilsby et al., 2007) is used for the re-parameterization of AWE-GEN-2d. The FC approach was chosen as it allows consideration of changes in the long-term mean, as well as changes in higher order statistics, and accounts for seasonality. FC are obtained by computing the difference between statistics of climate variables from a control realization and a future realization, originated from a specific GCM or RCM. The control realization (CON) is the period for which both observed data and climate model simulations are available, while the future realization (FUT) is the period for which only climate model simulations are available. FC can be applied at finer temporal scales than the scale of the original climate model, with the due attention to scale dependency and breaks in the higher order statistics (Marani, 2005; Bordoy and Burlando, 2014). FC can be a product factor (e.g. for

precipitation statistics), in such a case the ratio between statistics for FUT and CON realizations are used to modify the observed statistics as:

$$S(h)_v^{FUT} = \frac{S(h)_v^{CLM,FUT}}{S(h)_v^{CLM,CON}} S(h)_v^{OBS} \quad (1)$$

where $S$ is a statistical property (e.g. *mean*), $h$ is the time aggregation (e.g. *daily*), the subscript $v$ is the climate variable (e.g. *precipitation*), the superscript *FUT* and *CON* denote future and control realizations (respectively), *CLM* denotes the climate model (*RCM* or *GCM*), and *OBS* denotes the observed data. Alternatively, FC can be an additive factor (also known as Δ-change, e.g. for temperature statistics), in such a case the difference between statistics for FUT and CON realizations are used to modify the observed statistics as:

$$S(h)_v^{FUT} = S(h)_v^{OBS} + (S(h)_v^{CLM,FUT} - S(h)_v^{CLM,CON}) \quad (2)$$

with the same notations as above.

FC can theoretically be applied to every statistic of climate variables simulated by a climate model and used by AWE-GEN-2d for the parameter estimation. However, at present, the re-parameterization is applied only for a limited number of statistics characterizing the simulated cloud cover, precipitation and near-surface air temperature (Table 1), as these climate variables are among conventional outputs available from GCMs and RCMs and are arguably the most important for hydrological simulations. Additionally, once these climate variables are re-parameterized in AWE-GEN-2d, other variables are indirectly affected due to the dependencies between variables that are implemented in the model (Peleg et al., 2017b). For example, cloud cover controls the incoming shortwave radiation, and solar radiation and near-surface air temperature influence vapor pressure. The FC are calculated in this study on a 3-monthly basis to include the effects of intra-annual seasonality, but we note that they can be applied in several ways depending on the specific local climatology and on the research question in mind. For example, the model can be used to simulate a given climate trajectory by using FC that are obtained from a specific climate model (as demonstrated in the experiments described below), or, it can be used to simulate a multi-model ensemble by using a statistical approach (e.g. a Bayesian framework, see Fatichi et al., 2011; Tebaldi et al., 2005; Xu et al., 2018) to sample the FC obtained from multiple climate models. In the following paragraphs, details of the re-parameterization of different components of AWE-GEN-2d are provided.

The precipitation occurrence filter can be re-parameterized for a future climate if RCM results are available at a relatively high-resolution (e.g. with a spatial resolution of ~15 km or finer). Occurrence statistics are calculated for CON and FUT periods from the climate models and are linearly interpolated in space to match the grid cell resolution of AWE-GEN-2d. An additive FC is then applied to define the occurrence filter for FUT period. Concurrently, the GP distributions describing the precipitation intensity filter are re-parameterized for the future climate using product FC. The FC for the mean and variance of the precipitation intensities are calculated in each cell of the RCM, interpolated spatially and applied to the observed statistics. In such a way, the parameters of the GP distributions are re-estimated.

The parameters of the Johnson distribution that simulates the cloud cover during dry spells is re-parameterized for the future climate using product FC. As the Johnson distribution has more parameters than GP, we use higher order statistics to fit the new parameters and reduce the uncertainty of the fit. The FC for the mean, standard deviation, kurtosis and skewness of the cloud area ratio for the dry spells are calculated from RCM results and applied to the observed statistics. The parameters of the Johnson distribution are then re-fitted.

An additive FC [ΔT(t)] is used to modify near-surface air temperature for the future climate. This is applied directly to the mean near-surface air temperature over the entire domain.

### 2.3. Re-parameterizing statistics based on observed natural variability

The wet and dry spells are simulated in AWE-GEN-2d using a renewal process at a temporal resolution (hourly) that is finer than the temporal resolution of data saved in most GCMs and RCMs simulations (daily). Therefore, the parameters of the probability distributions used to simulate future wet/dry sequences cannot be directly re-parameterized by using information derived from the climate models. This means that we cannot use the FC approach for re-parameterizing the alternating renewal process for the future climate. Instead, we rely on observations and assume that climate change signals in the statistics of future wet/dry spells can be represented by the current variability of the observed wet/dry spells. Changes in the occurrence and duration of wet and dry spells were reported by many studies dealing with future climates (Heinrich and Gobiet, 2012; Peleg et al., 2015a; Svoboda et al., 2016) and projected changes in the sequences of future wet and dry spells are, in most cases, comparable to the observed natural variability (e.g. Peleg et al., 2015a).

To compute the observed variability in wet/dry spells, a bootstrap method (Efron, 1979) is used. Bootstrapping has been applied many times in the past to analyze natural variability (e.g. Alexander and Arblaster, 2009; Marra et al., 2017; Peleg et al., 2018). If the observed wet/dry sample is large enough (e.g. > 30-year of data), it can be re-sampled (with replacement) on an annual scale; meaning that a wet/dry sequence of a given year can appear several times in the new sample, or not at all. Once the new sample of wet/dry sequences is generated, new statistics and parameters for the probability distribution can be calculated. In this way, we consider the new set of parameters to represent a possible change in climate as we assume that the climate change signal (impossible to compute from climate models) is contained within the natural variability of the historical period. Then the stochastic nature of AWE-GEN-2d superposes a stochastic variability on top of this climate change signal as done for climate change signals directly derived through FC (e.g. mean air temperature) (Section 2.2).

## 3. Case study

### 3.1. Study area

The Engelberg region (Swiss Alps; 8.48 °E/46.88 °N) was chosen as a case study to demonstrate AWE-GEN-2d abilities to simulate an ensemble of climate variables for the period 2020–2089 and to discuss stochastic uncertainty over a typical size of a RCM grid cell (the domain scale of Engelberg area is 13 × 13 km$^2$) and at the local grid scale (2 × 2 km$^2$ or less) that is simulated using AWE-GEN-2d. The region is characterized by complex topography, with elevation ranging between 404 and 3119 m above sea level (Fig. 1). We used AWE-GEN-2d to simulate multiple climate variables for this region (precipitation, cloud cover, near-surface air temperature, solar radiation, vapor pressure and relative humidity), of which only precipitation and near-surface air temperature are discussed in the manuscript; the other climate variables are presented exclusively in the Supplementary Material.

AWE-GEN-2d was previously calibrated and validated for this region for present climate conditions (Peleg et al., 2017b), with 30 years of observations or more, according to the climatic variable. The wet and dry spell statistics, the spatial distribution of precipitation intensity and the variability of precipitation at different scales were examined, along with the diurnal cycle of near-surface air temperature, daily maximum, mean, and minimum temperature values and spatial distribution of temperature. It was concluded that precipitation, cloud cover (which is a closely related variable to precipitation) and near-surface air temperature variables are generated by AWE-GEN-2d with a high level of accuracy sufficient for most hydrological applications (Peleg et al., 2017b). The validation of the other climate variables is discussed in Section S1 (Supplementary Material).

The ability of AWE-GEN-2d to simulate the natural climate

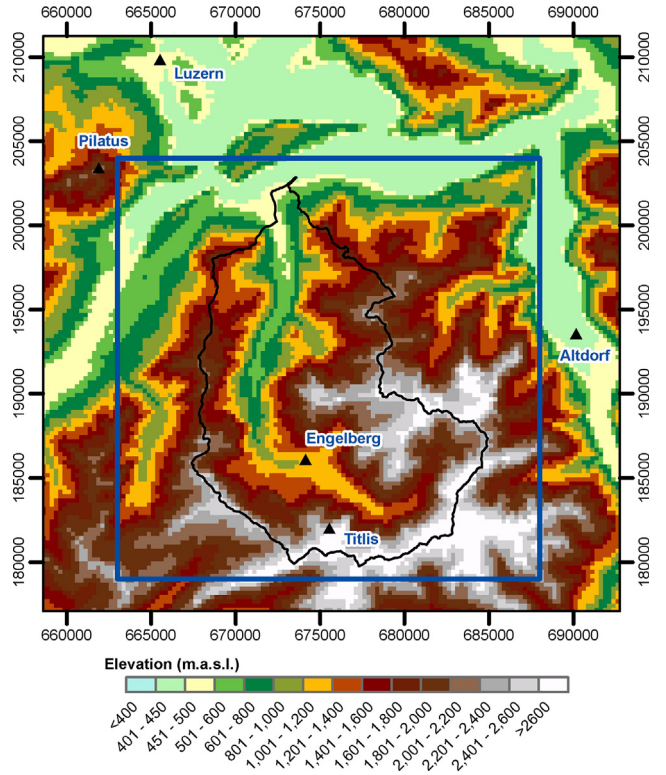


**Fig. 1.** Terrain map of the Engelberg region, Switzerland. The simulated domain is delimited by the blue square. The hydrological catchment is bounded with a black line. Black triangles represent meteorological stations in and around the catchment. CH1903 coordinate system (meters) is used. (For interpretation of the references to color in this figure legend, the reader is referred to the web version of this article.)

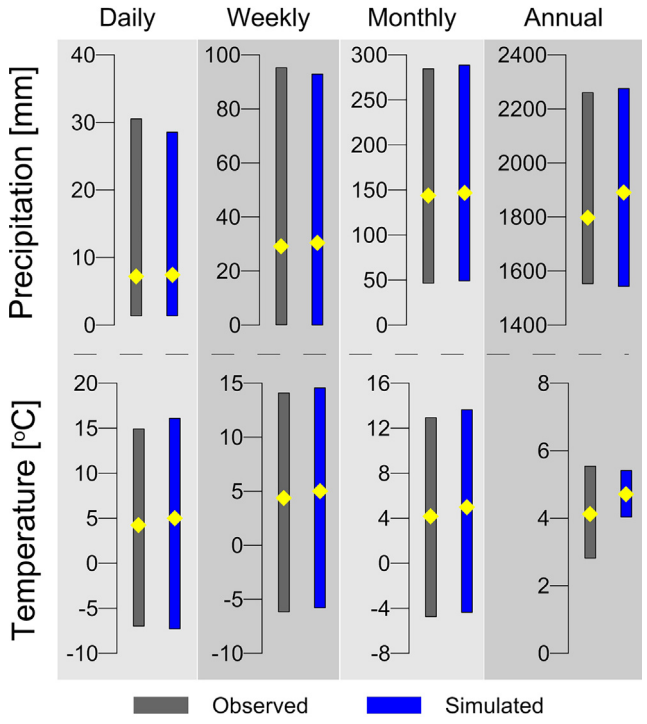


**Fig. 2.** A comparison between the estimates of the natural climate variability for the observed (grey) and simulated (blue) data for precipitation (upper part of the graph) and temperature (lower part) averaged over the Engelberg domain. The yellow diamonds represent the median values and the bars represent the 5th-95th percentile range. The statistics of daily rainfall are calculated only for days with rainfall exceeding 1 mm. (For interpretation of the references to color in this figure legend, the reader is referred to the web version of this article.)

variability of precipitation and temperature at different temporal scales over the domain is further examined here (Fig. 2). An ensemble of meteorological variables (hourly resolution) made of 30 realizations of 30 years each was simulated with AWE-GEN-2d and compared to an ensemble of the same dimension generated by bootstrapping the observed data but with daily resolution. The median and the 5th and 95th percentiles (a measure of variability) of daily precipitation for the 30-year period were calculated for each individual realization and, later, averaged. Observed and simulated data were aggregated to weekly, monthly and annual scales and the natural climate variability was computed at each scale. An identical methodology was applied to the near-surface air temperature data. The model satisfactory reproduces the natural climate variability at the daily to monthly scales both for precipitation (difference between the observed and simulated 5th-95th range are 2.3 mm at most) and temperature ($< 1.5\,^{\circ}C$) (Fig. 2). At the annual scale, the 5th-95th range of the simulated natural climate variability for precipitation is larger by 24.6 mm (or 3.4%) in comparison to the observed range, and smaller by 1.3 °C (50%) for temperature. The latter problem is expected and known as "overdispersion" (Fatichi et al., 2011; Katz and Parlange, 1998). For temperature the model simulates the periodic external forces (such as diurnal cycle and seasonality), but is not able to account for variations in the climate system due to large scale circulation patterns (e.g. variations in ocean heat content) or persistent anomalies in a given region that can modify considerably annual means. A similar issue should be expected for precipitation as well, if not properly addressed (Fatichi et al., 2011), but it is not evident from the obtained results.

Most of the climatic data for this region were supplied by the Swiss Federal Office for Meteorology and Climatology (MeteoSwiss) and from the MERRA re-analysis (Rienecker et al., 2011). Data products (details can be found in www.meteoswiss.admin.ch) include weather radar observations, gridded data products of precipitation and temperature (RhiresD and TabsY) and classic meteorological ground-stations (SwissMetNet) (Fig. 1). Further details on the data used to calibrate and validate AWE-GEN-2d for present climate conditions and their sources can be found in Peleg et al. (2017b).

### 3.2. Climate models and factors of change

Five RCMs from the EURO-CORDEX initiative (Giorgi et al., 2009; Kotlarski et al., 2014; Prein et al., 2016) were chosen for the re-parameterization of AWE-GEN-2d for future climate conditions (Table 2). The chosen RCMs have daily temporal resolution and spatial resolution of about 12 km (0.11°). The five models correspond to different GCM-RCM chains, chosen to minimize the potential effect of interdependence between climate models (Knutti et al., 2013) on the multi-model ensemble. For the presented case study, only the RCP8.5 emission scenario, characterized by the largest increase in global temperature and greenhouse gas concentration (Meinshausen et al., 2011) is considered. Cloud cover, precipitation and near-surface air temperature variables

**Table 2**
The five regional climate models used in this study, belonging to the EURO-CORDEX archive. The 'abbreviated as' column refers to the names used in this study.

| RCM | Driving GCM | Abbreviated as |
|---|---|---|
| CLMcom-CCLM4-8-17 | MOHC-HadGEM2-ES | CLMcom |
| DMI-HIRHAM5 | NCC-NorESM1-M | DMI |
| KNMI-RACMO22E | ICHEC-EC-EARTH | KNMI |
| MPI-CSC-REMO2009 | MPI-M-MPI-ESM-LR | MPI |
| SMHI-RCA4 | CNRM-CERFACS-CNRM-CM5 | SMHI |

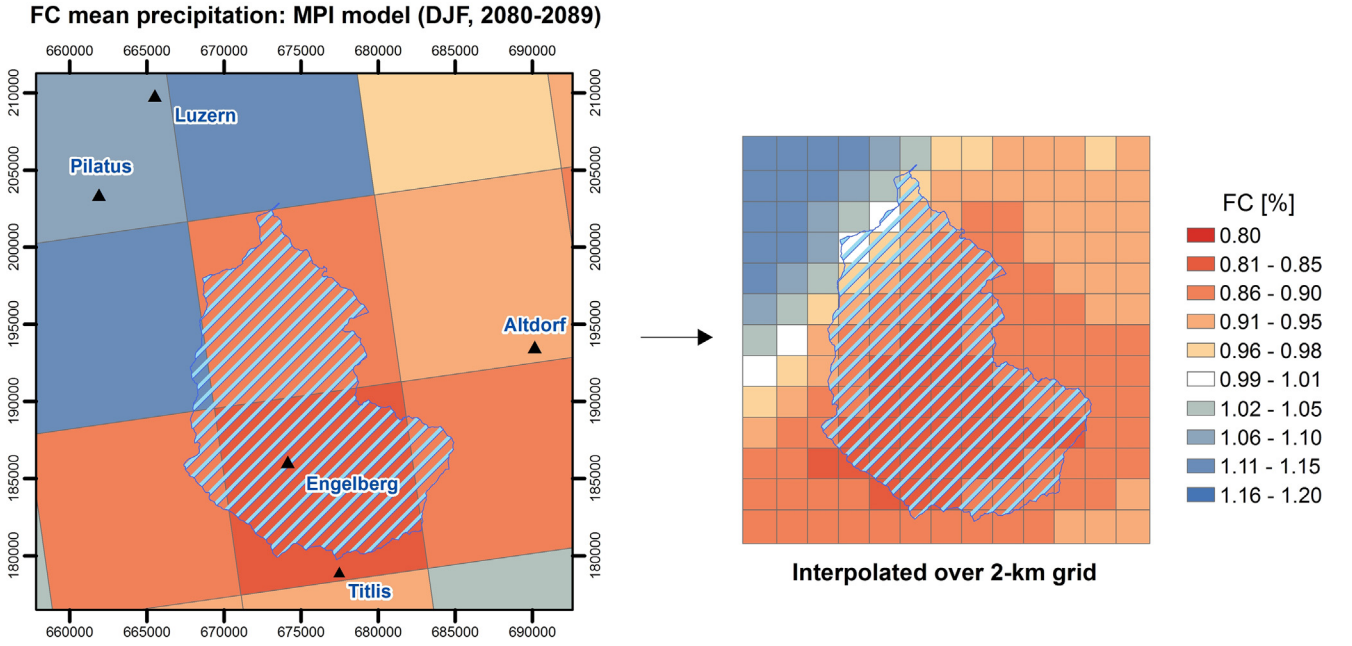


**Fig. 3.** An example of the spatial interpolation of FC from a RCM grid to the AWE-GEN-2d grid. Linear interpolation in two-dimensions was used to transform FC for mean precipitation from the 12-km resolution of the climate model grid (MPI) to the 2-km resolution Cartesian grid of AWE-GEN-2d for the Engelberg area.

for the 'historical' (1970–2005) and 'future' (2006–2100) periods were used.

FC (Table 1) were calculated over the RCMs grid, and then they were spatially interpolated to the Cartesian grid of AWE-GEN-2d using a 2-dimensional linear interpolation (Fig. 3). The FC were calculated on seasonal basis for each decade using a 30-year moving time window, since 30 years are necessary for computing statistics (see further explanation in Section 4).

The FC for precipitation statistics were computed for changes in the mean (Fig. 4), occurrence (Fig. S1), and standard deviation (Fig. S2). Differences are evident between decades and among the five climate models. In general, changes are more prominent toward the end of the century for all statistics. The spatial pattern of the FC of precipitation mean (Fig. 4) and standard deviation (Fig. S2) is quite similar. There is, however, no consensus between climate models when FC of precipitation mean (Fig. 4) and occurrence (Fig. S1) are jointly considered. For example, both FC of precipitation mean computed from MPI and KNMI models for JJA for the end of the century are indicating a general reduction in precipitation intensity, while the FC of precipitation occurrence are pointing to both a decrease (MPI) or increase (KNMI). Seasonally, the FC of precipitation mean are sometimes found to be larger than 1.25; (CLMcom, DJF, end of the century) or smaller than 0.80 (MPI, JJA, end of the century), but at the annual scale the FC of precipitation mean are rarely exceeding the ± 10% range.

No clear trends were found for cloud cover changes for both near (2020–2029) or far (2089–2089) futures (Fig. 5). The FC for cloud cover mean are changing between seasons, climate models or decades but without any apparent pattern. Most FC for cloud cover mean were found to be within a ± 5% range, thus making it impossible to judge if the difference represents a climate change signal or it is stochastic noise. FC derived from the CLMcom climate model yield a substantial cloud cover reduction by the end of the century, e.g. 10% and 22% reduction in cloud cover mean for SON and JJA (respectively). However, these results were considered unrealistic (for example, Bartók et al. (2017) indicated that changes in annual cloud cover for this region do not exceed 8%) and these FC values were omitted for the subsequent re-parameterization of AWE-GEN-2d.

A clear signal of increase in near-surface air temperature is projected from all models, as evident from the FC for temperature mean (Fig. 6). The spread in FC is relatively high for the end of the century and changes in temperature range between 2.75 °C (DMI model) and 4.5 °C (SMHI model), when computing the FC at the annual scale. Model spread in FC is higher for DJF and MAM in comparison to JJA and SON.

## 4. Experimental setup

Weather generators can be used to simulate future climate scenarios for a long continuous period (non-stationary approach) considering the transient nature of the climate change signals (e.g. Blenkinsop et al., 2013; Burton et al., 2010; Glenis et al., 2015), or to simulate a given period (usually 20–30 years long) under the assumption of stationarity, i.e. considering that the climate change signal is constant during this period (e.g. Camici et al., 2014; Fatichi et al., 2013, 2015; Peleg et al., 2015b; Singer and Michaelides, 2017; Singer et al., 2018).

Two experiments were conducted for the case study area. In the first experiment, a transient multi-model ensemble was generated for the period 2020–2089. The FC are calculated based on a 30-year moving window (a typical interval used to define climatological values according to the World Meteorological Organization) and are updated every decade (Fig. 7). Each decade is simulated using a new set of FC that covers the preceding and following decades. We note that the computation of FC can be sensitive to the size of the moving window but 30 years is long enough to guarantee a smooth transition between decades. The first experiment allows the detection of the time when the signal of climate change is, if at all, greater than the natural (stochastic) variability of climate. Moreover, it is a demonstration of AWE-GEN-2d ability to generate climate variables for a long and continuous period in the future. In this experiment, precipitation, cloud cover, near-surface air temperature, incoming shortwave radiation, vapor pressure and relative humidity variables from annual to hourly scale and from domain to individual grid cell scale were explored. The new sets of parameters for AWE-GEN-2d were estimated on a decadal basis, as illustrated in Fig. 7 and explained above. In total, 3500 years were generated (5 driving RCMs × 7 decades × 10 stochastic realizations).

The second stationary experiment was designed to explore the stochastic uncertainty at the domain scale (13 × 13 $km^2$) and at the scale of a single grid cell (2 × 2 $km^2$ for precipitation and 100 × 100 $m^2$ for

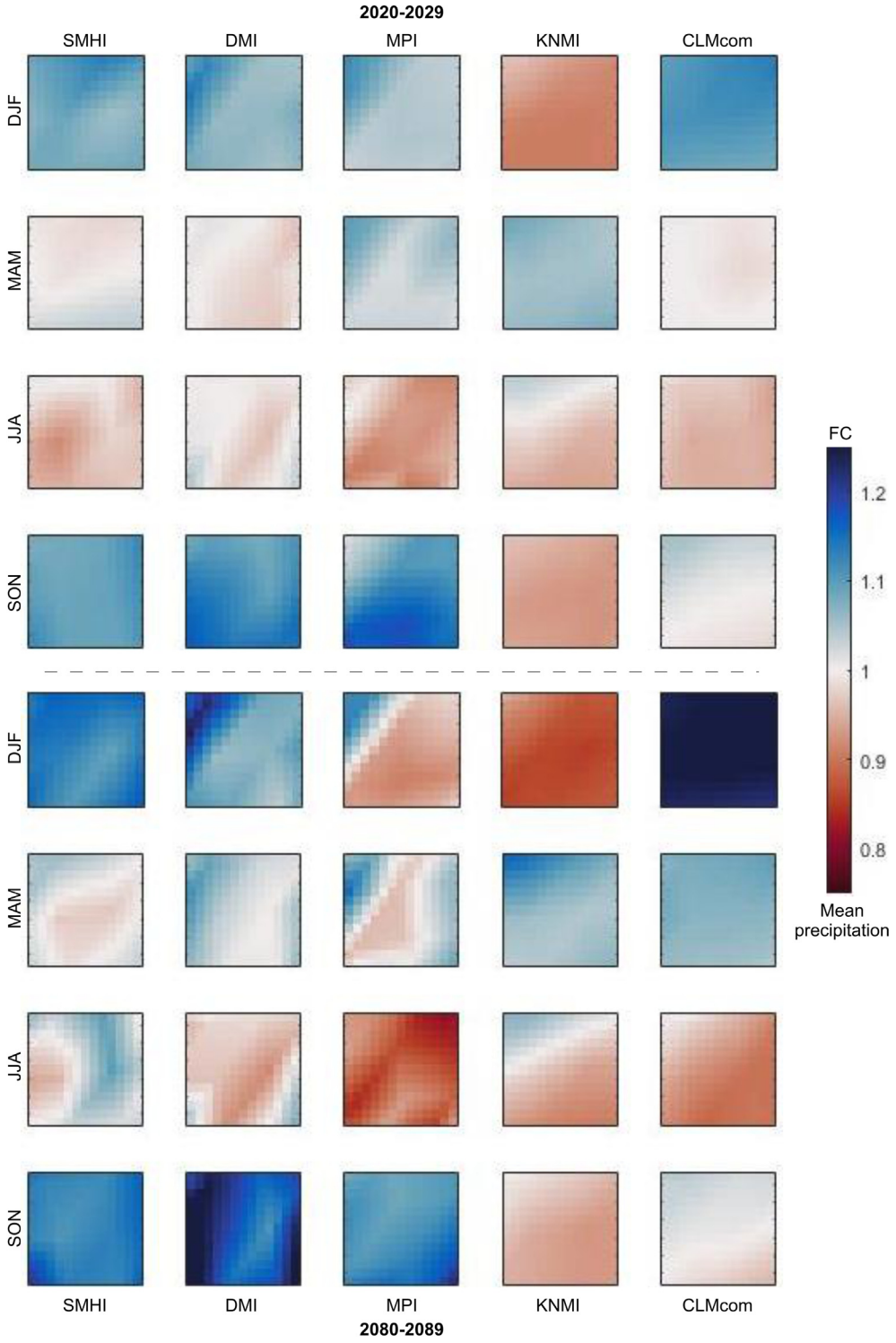


**Fig. 4.** Ratio FC for precipitation mean in the study domain calculated for the decades 2020–2029 (above the dashed line) and 2080–2089 (below the dashed line) using five RCMs (columns) and on a seasonal basis (rows).

near-surface air temperature) for the control and future periods. A new ensemble of 900 years (equivalent to 30 realizations of 30 years each) was simulated only for the period 2070–2099. The ensemble was then bootstrapped to form 1000 realizations of 30 years each. The re-parameterization set of the 2080–2089 decade from the first experiment was used for this purpose, as the data from the climate models used for this period are representative of the period of interest (see illustration in Fig. 7). A similar ensemble was simulated for the control period. For this specific experiment, only the FC obtained from a single RCM model (KNMI as a representative example) were used, in order to single out the role of stochastic uncertainty without the confounding role of different climate models. This second experiment focuses on precipitation and near-surface air temperature, as they are the most important climate variables for hydrological applications. For each of the simulated realizations, the mean annual precipitation of the 30-year period was calculated. The stochastic uncertainty of the annual precipitation was then computed as the difference between the 5th and 95th percentiles of the 30-year mean annual precipitation of the 1000 members of the

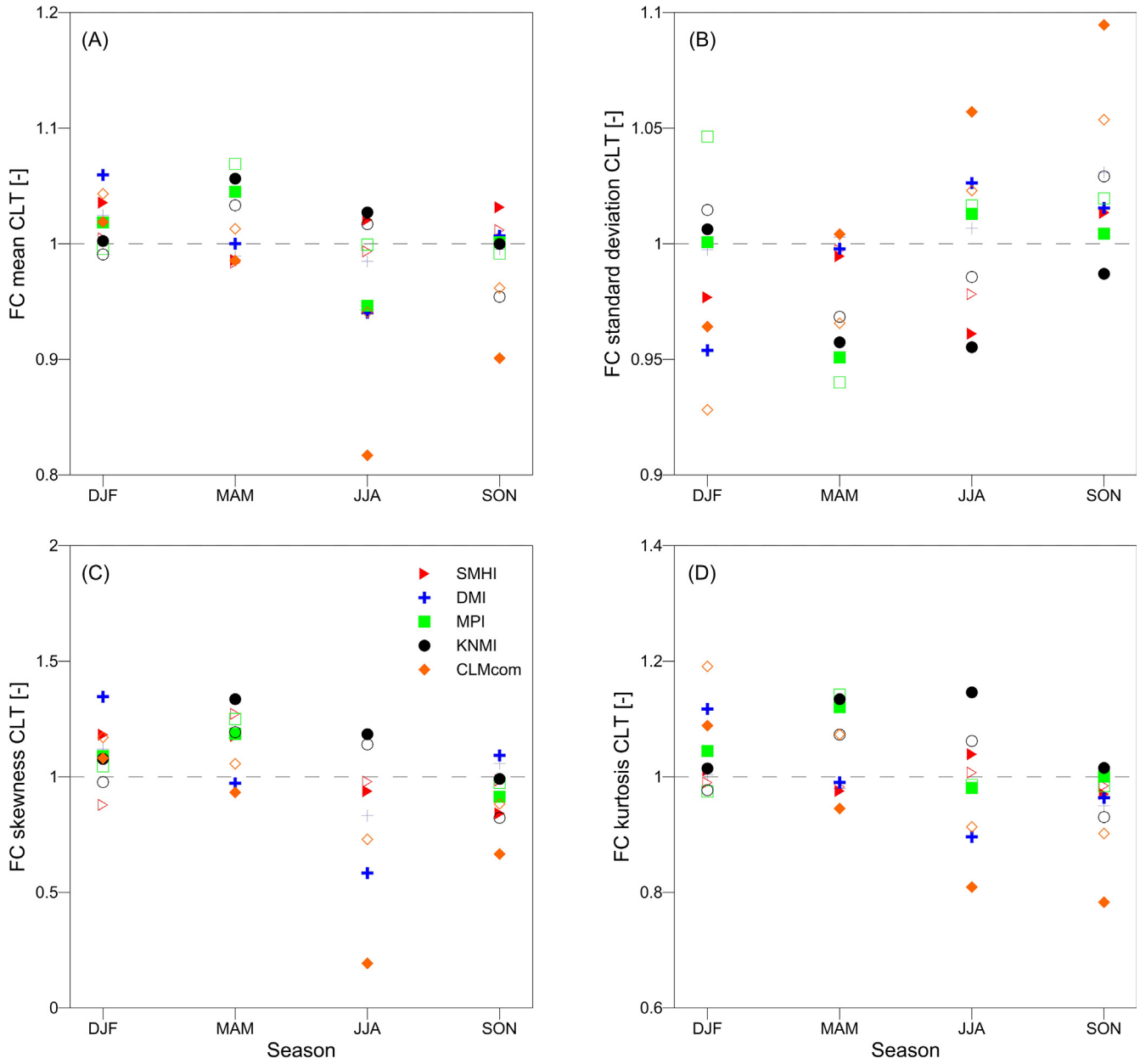


**Fig. 5.** Ratio FC for cloud cover mean (A), standard deviation (B), skewness (C) and kurtosis (D) statistics are calculated for the decades 2020–2029 (empty symbols) and 2080–2089 (filled symbols) using five RCMs (different symbols). The FC are calculated on a seasonal basis and are averaged over the domain.

ensemble. The stochastic uncertainty can then be normalized by the median of the annual precipitation to allow a better comparison between the two spatial scales and the different periods. The same procedure was conducted for the near-surface air temperature, but in this case the 5th-95th percentile range is not divided by median. Using the same approach, the stochastic uncertainty of the daily extreme precipitation intensity was also explored. The daily extreme precipitation intensity was computed for the 2-, 10- and 30-year return periods using the annual maxima method (as in Marra et al., 2017; Peleg et al., 2018).

## 5. Results

All climate variables were generated at the hourly scale. Precipitation and cloud cover are generated over a $2 \times 2\,km^2$ grid (similar to the resolution of the weather radar inputs), while the other climate variables (near-surface air temperature, solar radiation, vapor pressure and relative humidity) are generated at a finer resolution of $100 \times 100\,m^2$, thus accounting for topographic features. Results of the first experiment for precipitation, cloud cover and near-surface air temperature are presented in the following subsection, while results for incoming shortwave radiation, vapor pressure and relative humidity are given in the Supplementary Information (Section S3, Fig. S8-S11). Changes are expressed as differences between AWE-GEN-2d generated climate variables for present and future conditions.

### 5.1. First experiment

Changes in precipitation are first analyzed at the areal (i.e. for the entire domain) and annual scales. The simulated mean annual areal precipitation over Engelberg for the control period is 1896 mm, which is very similar to the multi-model mean (including 5 climate models and 10 stochastic realizations generated for each model) for the future climate (Fig. 8). The multi-model mean is monotonically increasing from 1934 mm (2% increase in comparison to the control period) for

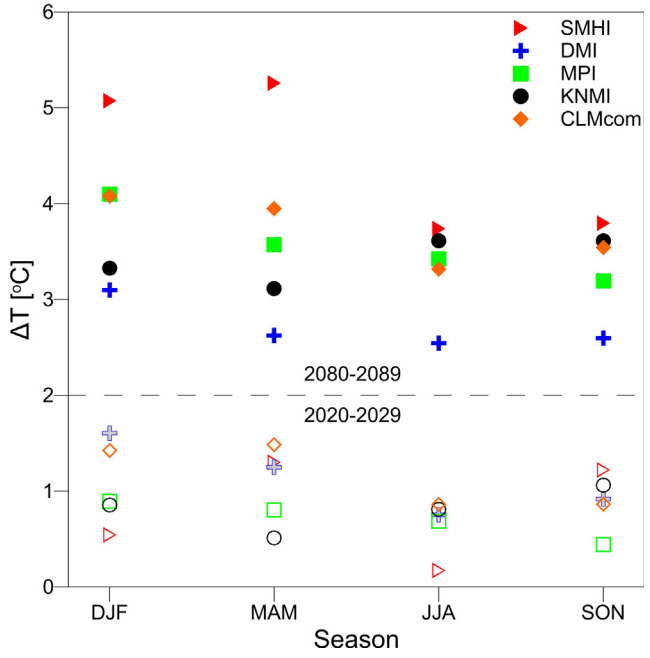


**Fig. 6.** Additive FC for near-surface air temperature mean calculated for the decades 2020–2029 (empty symbols) and 2080–2089 (filled symbols) using five RCMs (different symbols). The FC are calculated on a seasonal basis and are averaged over the domain.

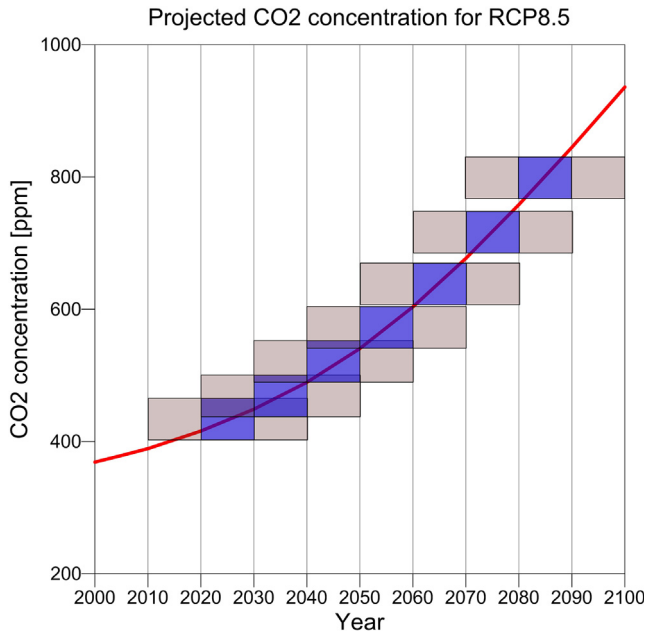


**Fig. 7.** A schematic illustration showing the projected $CO_2$ concentration for RCP8.5 (red line, following (Meinshausen et al., 2011)) and decadal periods (blue areas) of reference for which FC are estimated on a 30-year moving window centered in that period (grey areas) from the climate model outputs. (For interpretation of the references to color in this figure legend, the reader is referred to the web version of this article.)

the period 2020–2029 to 1968 mm (3.8% increase) at the end of the century (2080–2089). Some of the realizations driven by specific RCMs are showing lower mean annual areal precipitation compared to the control scenario (e.g. KNMI-driven simulations), some do not have any significant change (e.g. CLMcom) and some produce an increase in precipitation larger than the median (e.g. SMHI) (Fig. 8). The combination of precipitation FC for occurrence, mean, and standard deviation generates spatially heterogeneous changes (Fig. S3). The multi-model mean increase for most grid cells in the domain hardly exceeds 5% in comparison to the control period and larger changes occur in cells with lower mean precipitation; this is true for all the decades that were examined (Fig. 9). The changes for the hourly precipitation intensity were also examined for 6 exemplary grid cells (Fig. S3) and are presented in Fig. S4, showing a general intensification of the hourly precipitation by the end of the century.

There is basically no difference between the cloud cover simulated using AWE-GEN-2d for the control and future periods (Fig. S5 and S6). The simulated mean annual cloud cover for the control period is 58%, while the simulated multi-model means for the future vary between 58.5% and 59.5%, with no clear temporal trend. In general, cloud cover simulations show consistency among decades, both for the annual mean (Fig. S5) and for the hourly distribution (Fig. S6).

The AWE-GEN-2d simulations of near-surface air temperature over the Engelberg area show a considerable increase toward the end of the century. For the first simulated decade (2020–2029), an increase in average near-surface air temperature of 0.5–1.35 °C is projected in comparison to the control period (Fig. 10). The uncertainty mostly emerges from the climate model forcing (i.e. the difference between the FC obtained from the 5 RCMs) and is increasing towards the end of the century. For the last decade (2080–2089), an increase in average near-surface air temperature of 2.5–4.7 °C is simulated in comparison to the control period. The changes in near-surface air temperature, as simulated by AWE-GEN-2d, are homogenous in space, i.e. grid cells located at bottom of the valley or along mountain slopes show almost equal temperature changes (see example in Fig. 11). This is due to the fact that the temperature lapse rates are not re-parameterized and only spatially homogenous FC are applied. Changes in the cloudiness have the potential to spatially modify changes in the near-surface air temperature, but spatial variability of changes in near-surface air temperature due to the cloudiness was found to be very small in the Engelberg area, in the order of 0.01 °C, for simulations at the end of the century (Fig. 11). The diurnal cycle of the near-surface air temperature is, in fact, uniformly shifted (Fig. S7) and the simulated dynamics of the temperature diurnal cycle for the future climate are similar to the control period.

### 5.2. Second experiment

The stochastic uncertainty (30 realizations of 30 years) of the annual precipitation at the grid cell scale on average was found to be slightly higher in comparison to the stochastic uncertainty at the domain scale for the control period (7.5% and 7%, respectively) and in the future period (8.1% and 7.6%, respectively) (Fig. 12A). This tendency is expected since stochastic uncertainty should decrease as averages are taken over a larger area but absolute differences are minimal despite a forty times larger area. The stochastic uncertainty at the individual grid cells was found to vary between 7.1% and 8.9% for the control period, and between 7.6% and 9.4% for the future period (Fig. 12A). The stochastic uncertainty at the domain and grid cell scale for the daily precipitation extremes for the control and future periods is presented in Fig. 12B. As expected, the stochastic uncertainty increases when moving toward lower frequency extremes. For example, at the domain scale and for the future, the stochastic uncertainty increases from 16.4% for the 2-year return period to 22.1% and 23.9% for the 10- and 30-year return periods, respectively. The stochastic uncertainties at the grid cell scale are higher in comparison to those at the domain scale. For example, for the 10-year return period (control scenario), the stochastic uncertainty at the domain scale was 20.1% with a median precipitation intensity of 67.7 mm $d^{-1}$, in comparison to 32.5% uncertainty and 102.6 mm $d^{-1}$ median intensity at the grid scale. Finally, we can note that the stochastic uncertainty of the precipitation extremes has a similar range when we compare the control and future periods. For example, for the 10-year return period at the domain scale,

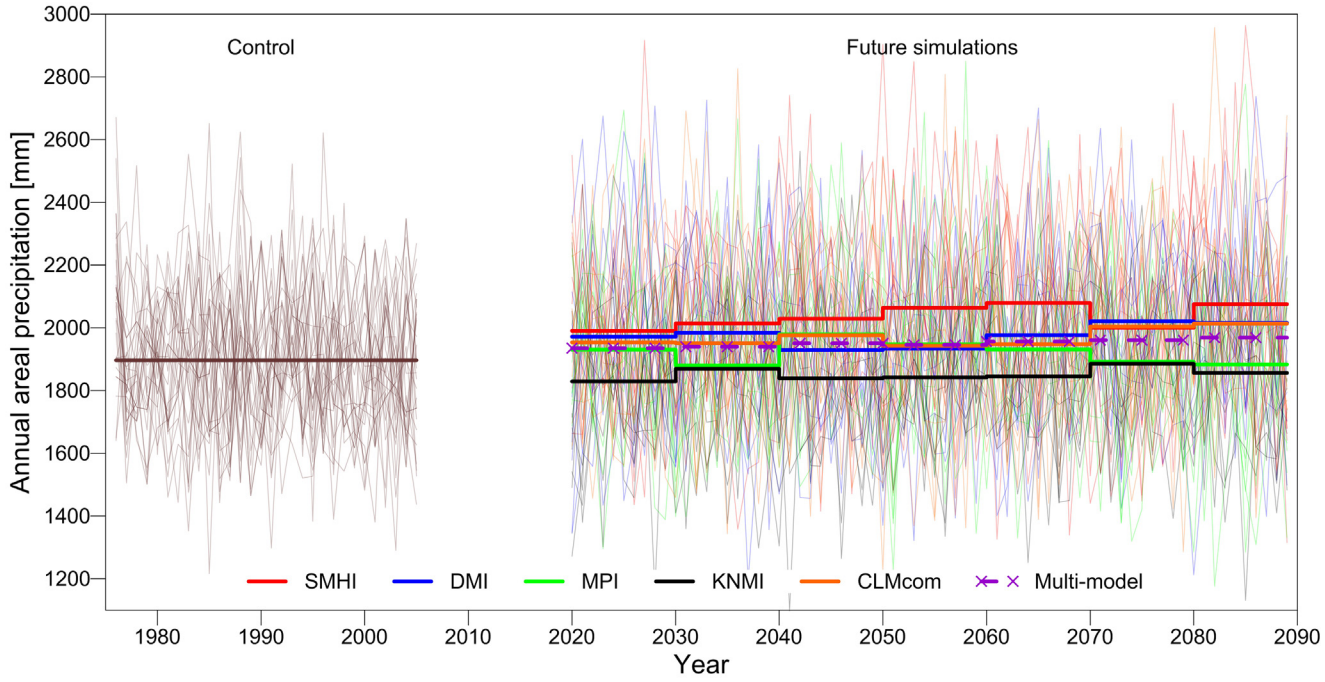


**Fig. 8.** Time series of annual areal precipitation over Engelberg region as simulated using AWE-GEN-2d for the control period (1976–2005, 30 realizations, brown lines) and the future period (2020–2089, 10 realizations per climate model, colored lines for each climate model forcing). Thick lines represent decadal mean and dashed line represents the multi-model mean.

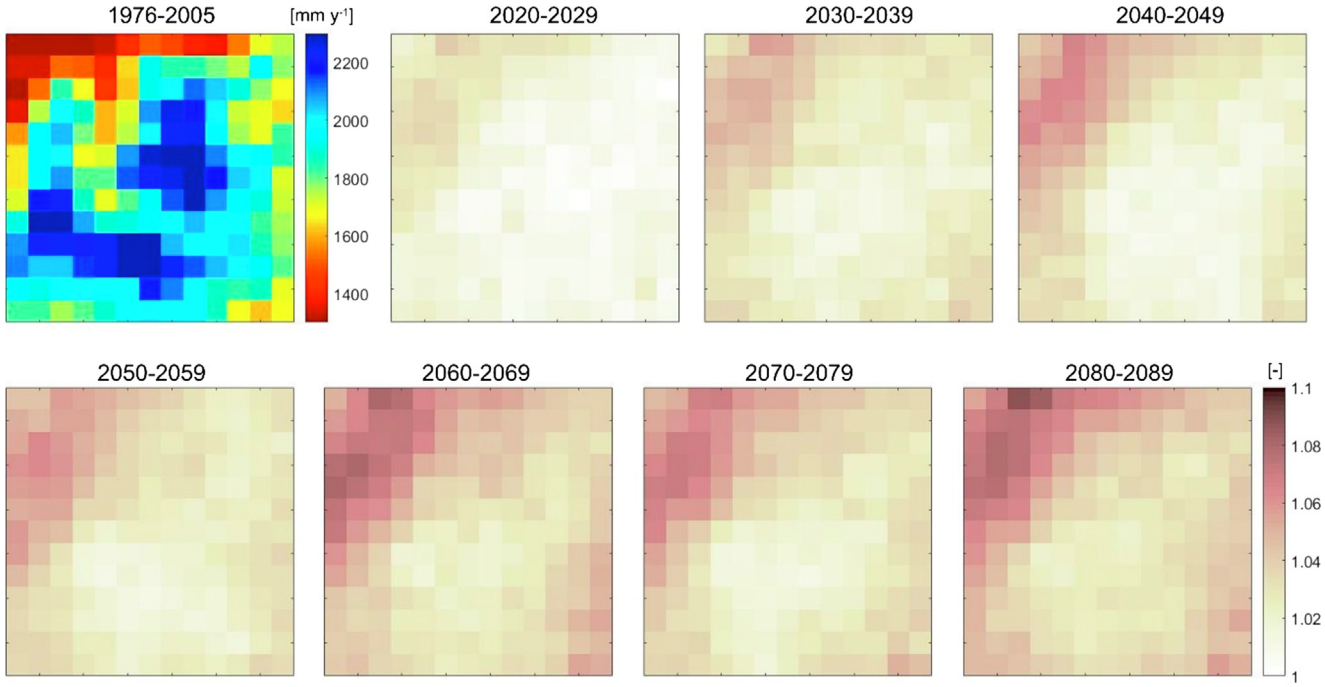


**Fig. 9.** The mean annual precipitation for the control period (1976–2005), generated using 30 realizations of 30 years each (top left). The multi-model mean annual precipitation for the future periods divided by the mean annual precipitation for the control period (other subplots). The multi-model mean annual precipitation for the future periods was generated using 10 realizations of 10 years for each of the FC sets derived from 5 RCMs (50 realizations per decade in total).

the stochastic uncertainty of the control period is 20.1%, and for the future period is 22.1%.

The stochastic uncertainty of the near-surface air temperature was also examined. It was found to have a very similar magnitude when comparing the grid cell and domain scales for the control and future periods. At the domain scale, the stochastic uncertainty was found to be 0.25 °C for both periods (Fig. 13). The stochastic uncertainty of the individual grid cells is deviating by less than 0.005 °C from the stochastic uncertainty of the domain (Fig. 13).

## 6. Discussion

### 6.1. The role of stochastic uncertainty across spatial scales

Climate outputs from GCMs and RCMs cannot be used directly as inputs into hydrological models in most studies, due to their coarse

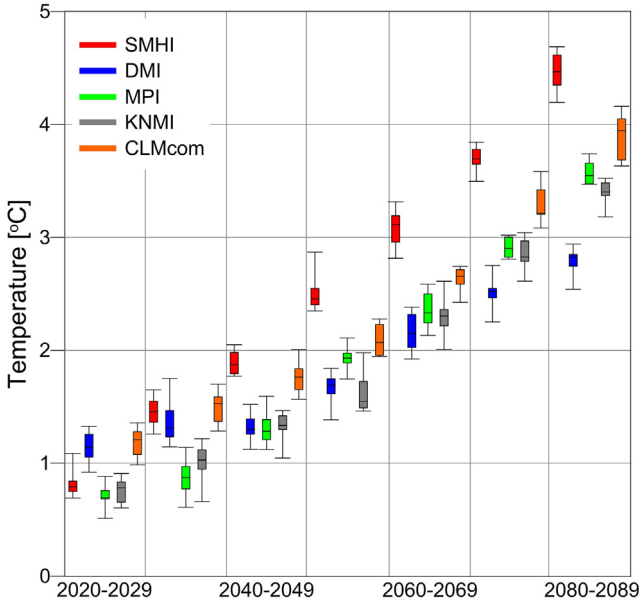


**Fig. 10.** Box-Whisker plot displaying the 5th-95th percentile range (whisker lines), lower and upper quartiles (boxed area) and median (black line) for the change in average near-surface air temperature over Engelberg area in comparison to the control period. Boxes represent the statistics of 10 realizations per decade that were simulated using AWE-GEN-2d driven by the additive temperature FC from 5 RCMs (unique color for each).

spatial and temporal resolution (often > 25 km and daily, respectively). Studies for catchments smaller than 10,000 $km^2$ often require climatic forcing at higher spatial and temporal resolution – e.g. at the kilometer or less and hourly scales. Moreover, distributed hydrological models, such as tRIBS (Ivanov et al., 2004), Topkapi-ETH (Fatichi et al., 2015), WaSiM (Schulla and Jasper, 2007), GEOtop (Endrizzi et al., 2014), or Parflow (Condon and Maxwell, 2015), require gridded climatic data as inputs, thus downscaling GCM/RCMs realizations to individual stations may be insufficient. Furthermore, downscaling one or few realizations of climate models is a common practice but could be quite misleading since it neglects internal climate variability (Deser et al., 2012b, 2014; Fatichi et al., 2016a; Sexton and Harris, 2015). Generating many climatic realizations is fundamental when exploring uncertainties, as the relative contribution of stochastic uncertainty to the total uncertainty of climate change projections is large at fine spatial scales, especially for precipitation (Fatichi et al., 2016a).

The advantages of stochastically downscaled climate variables at high spatial (gridded, kilometer scale) and temporal (sub-daily) resolutions are demonstrated in the results presented here. When AWE-GEN-2d was used to simulate the future climate for a long continuous period of 80 years, the multi-model mean for future precipitation at the domain scale increased in comparison to the control period by up to 3.8% (Fig. 8). However, this increase remains well within the range of the stochastic uncertainty of 30-year mean precipitation, which was found to vary between 7 and 7.6% (control and future periods, Fig. 12A). When examining individual grid cells, starting from 2060 to 2069, a few grid cells show an increase in mean annual precipitation of more than 8% (Fig. 9), meaning that their signal of change is greater than what would be expected from natural variability alone. However, these grid cells cover less than 10% of the domain. Although future daily extreme precipitation is projected to increase slightly in comparison to present extremes, the change is also well within the stochastic uncertainty (Fig. 12B). On the contrary, changes in near-surface air temperature are exceeding the stochastic uncertainty at the domain and individual grid cell scales, which is 0.25 °C (Fig. 13), starting already from the near-future 2020–2029 (multi-model mean increase of 1 °C in comparison to the control period, Fig. 10). The small changes in future cloud cover (~1%, Fig. S5) lead to minor changes in radiation and relative humidity (e.g. < 0.5 $W m^{-2}$ change in the incoming shortwave radiation at the annual scale, Fig S8) and to considerable changes in vapor pressure (up to 30%, Fig. S10). We can therefore conclude from this analysis, carried out for the Engelberg region, but eventually exemplary for prealpine and alpine regions, that significant changes are expected for near-surface air temperature and vapor pressure, while statistics of the other climate variables are likely to remain largely within the range of present natural variability.

Generally speaking, the stochastic uncertainty of climate variables is expected to increase moving towards finer spatial scales (Fatichi et al., 2016a; Hawkins and Sutton, 2011). We observe such a pattern for precipitation, for which our results indicate that the stochastic uncertainty at the domain scale (13 × 13 $km^2$) is slightly lower than the stochastic uncertainty at the scale of the individual grid cells (2 × 2 $km^2$) (Fig. 12A). However, the difference is smaller than we expected, in the order of 0.5%, and unlikely to be of any practical significance. This suggests that stochastic variability may be a dominant factor for precipitation projections not only at the local scale (Fatichi et al., 2016a) but also at scales typical of RCM/GCM grid cells and potentially even at larger scales. As a matter of fact, the role of internal climate variability has been found to be important for precipitation also at continental scale (Deser et al., 2012b; Hawkins and Sutton, 2011). For near-surface air temperature there is practically no difference between the stochastic uncertainties at the different scales (Fig. 13), but as explained earlier, this uncertainty is much smaller than the climate

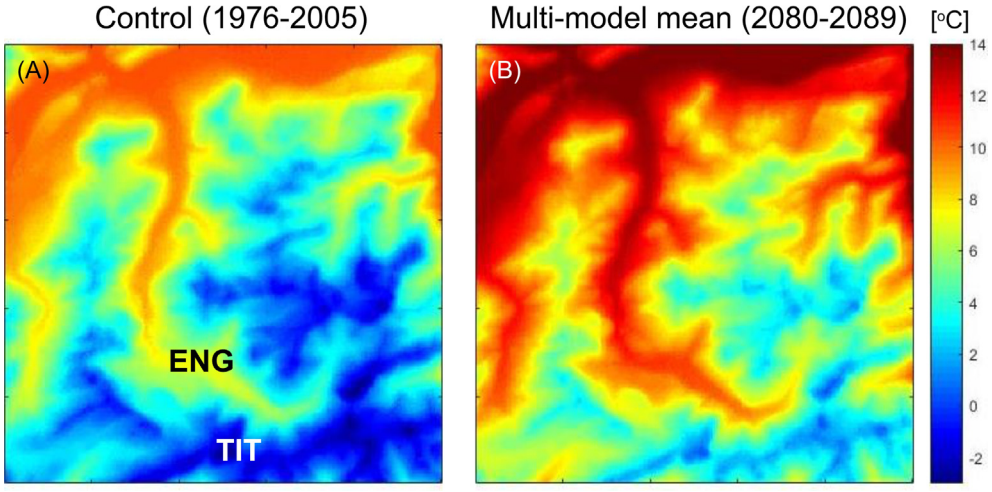


**Fig. 11.** The mean annual near-surface air temperature for the control period (1976–2005), generated using 30 realizations of 30 years each (A); and the multi-model mean annual near-surface air temperature for the end of the century (2080–2089), generated using 10 realizations of 10 years each using 5 driving RCMs (B). 'ENG' and 'TIT' mark the locations of Engelberg and Titlis stations (respectively).

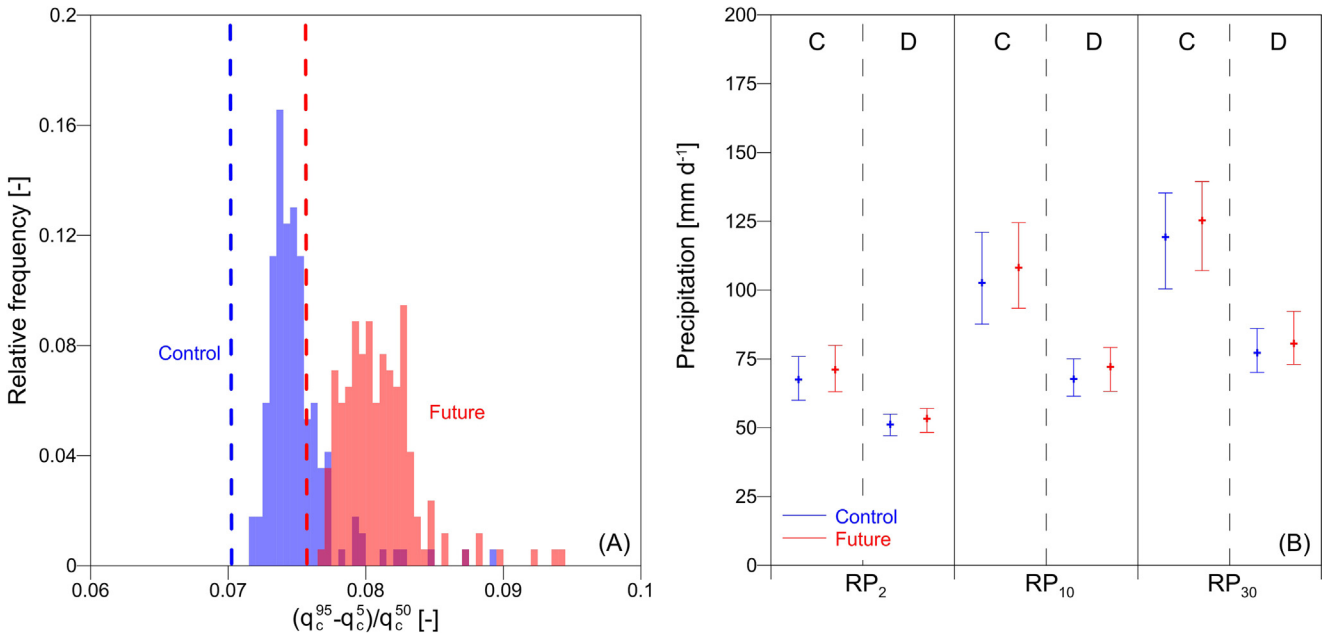


**Fig. 12.** (A) A comparison between the distribution of the stochastic uncertainty (5th-95th percentile) of annual precipitation for the control (blue) and future (red) periods at the grid cell scale. Note that the stochastic uncertainty of each grid cell is divided by the median. Solid lines represent the stochastic uncertainty of annual precipitation at the grid cell scale and dashed lines represent the stochastic uncertainty at the domain scale. (B) A comparison between the stochastic uncertainty of daily extreme precipitation for the 2-, 10- and 30-year return period ('$RP_2$', '$RP_{10}$', and '$RP_{30}$', respectively) for the control (1976–2005, blue) and future (2070–2099, red) periods. Lines represent the 5th-95th percentile range and dots represent the median of the data obtained from 30 realizations of 30 years each. 'C' stands for the grid cell scale ($2 \times 2\,km^2$) and 'D' for domain scale ($13 \times 13\,km^2$). (For interpretation of the references to color in this figure legend, the reader is referred to the web version of this article.)

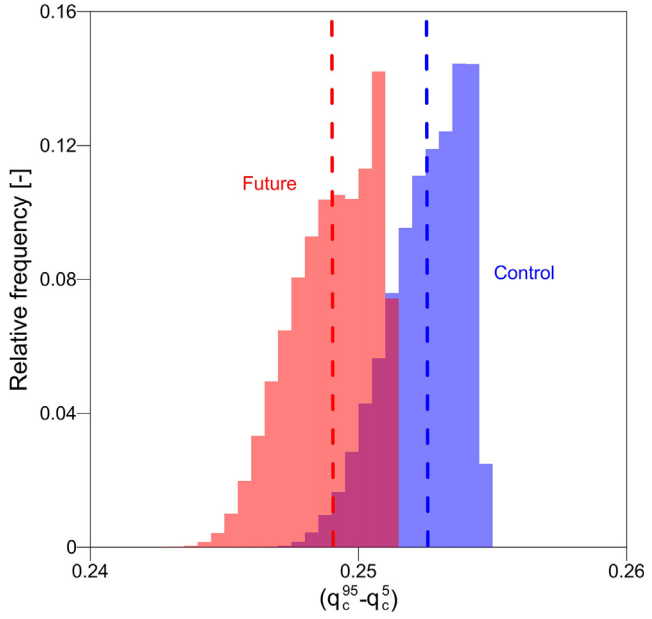


**Fig. 13.** A comparison between the distribution of the stochastic uncertainty of annual temperature for the control (blue) and future (red) periods at the grid cell scale. Dashed lines represent the stochastic uncertainty of annual temperature at the domain scale. (For interpretation of the references to color in this figure legend, the reader is referred to the web version of this article.)

change signal. Overall, it is likely that estimating the stochastic uncertainty at the local scale (station level) may provide a good estimate of uncertainty at the climate model scale (12-km for some of the EURO-CORDEX models) and probably even at larger scales, even though this remains to be tested.

### 6.2. AWE-GEN-2d and future climate projections

AWE-GEN-2d is a statistical-stochastic weather generator, and as such it has some limitations when simulating climate variables for the future. Parameters are calibrated based on statistics obtained from observed data that are perturbed with information derived from climate models. These modified statistics are then used to estimate new sets of parameters. Unfortunately, only a few statistics needed to properly re-parameterize the WGs are derivable from currently available GCM/RCM outputs. Inferring changes in other statistics would require sub-daily or/and gridded climate model outputs at the kilometer scale. For example, this resolution would be necessary to modify the statistics of the diurnal cycle of temperature or to modify the precipitation spatial structure. Moreover, some of the data that is used for the calibration of the model, such as ozone and nitrogen dioxide amounts in the atmosphere or information on the aerosol optical depth that are used for the calibration of the radiation components (Peleg et al., 2017b) are simply not available in common GCM/RCM outputs. AWE-GEN-2d parameters that are not modified for the future climate simulations, such as the statistics of wet and dry spells and the tri-variate process that is used for the simulation of the areal statistics of each storm (precipitation areal intensity, wet area ratio and cloud cover ratio) were used with the same parameter set of the present climate. Yet, theoretically all these parameters in AWE-GEN-2d could be re-computed in future studies, depending on the availability of high-resolution (i.e. single run, hourly- and km-scale) simulations from the climate models.

While in the presented case study we restricted the number of simulations to the minimum that is sufficient to demonstrate AWE-GEN-2d capabilities and to explore climate and stochastic uncertainties, it is advisable to use as many climate models as possible to better capture climate model uncertainty, and it is recommended to simulate at least 50 realizations per climate trajectory to compute stochastic uncertainty as a good compromise between computational requirements and representativeness of stochastic uncertainty (Fatichi et al., 2016a; Kim et al., 2016; Peleg et al., 2017b).

Despite these limitations, which are partially related to AWE-GEN-2d and mostly to current availability of climate model outputs, the model is a very useful tool to explore stochastic climate variability at the climate model sub-grid scale. AWE-GEN-2d is parsimonious in terms of computational demands and can be run on a high-end desktop computer, without the needs of accessing high-performance computational centers. It allows downscaling and simulating multiple realizations of future climate and presents an attractive alternative tool to physically-based models for downscaling gridded climatic variables that are needed as inputs for hydrological applications. This is especially true when the major interest is to have a good representation of the natural climate variability, which we showed to be extremely important for precipitation not only at the station level but also at the scale of a climate model grid.

## 7. Summary

AWE-GEN-2d is a stochastic grid-based weather generator that simulates main climatic variables needed for hydrological modeling (i.e. precipitation, cloud cover, near-surface air temperature, incoming shortwave radiation, vapor pressure, and relative humidity) at sub-daily temporal and kilometer spatial resolutions. A methodology to re-parameterize AWE-GEN-2d using information from climate models (such as GCMs or RCMs) and to simulate variables representative of a future climate is presented for the statistics of cloud cover, precipitation and near-surface air temperature. The re-parameterization scheme and the assumptions made are described together with the benefits and limitations of using such a high-resolution space-time stochastic weather generator.

Climate change projections are derived for a mountainous area in the Swiss Alps to demonstrate the use of AWE-GEN-2d. It was found that the future climate for this region will be characterized by a considerable change in the statistics of near-surface air temperature and vapor pressure, while statistics of the other climate variables, such as precipitation, cloud cover and shortwave incoming radiation, are likely to remain within the range of stochastic (natural) climate variability. Stochastic climate uncertainty generated by AWE-GEN-2D was found to be very similar when comparing present and future periods and different spatial scales ($13 \times 13\,km^2$ and $2 \times 2\,km^2$). Simulating the stochastic climate uncertainty is fundamental for studies aimed at exploring the propagation of uncertainty in climatic forcing into other hydrological variables like evapotranspiration, snow cover dynamics or runoff. AWE-GEN-2d is a very suitable tool for providing climatic inputs to hydrological models for such tasks.

## 8. Code availability

The MATLAB source code of AWE-GEN-2d and the data used for the Engelberg case study are available upon request. Any element of AWE-GEN-2d is free to use, modify, copy or distribute provided it is for academic use and source code developers are properly acknowledged and cited.

## Conflicts of interest

The authors declare that there are no known conflicts of interest.

## Acknowledgements

This project is funded by the Swiss Competence Center for Energy Research-Supply of Electricity (http://www.sccer-soe.ch). We thank the EURO-CORDEX initiative for supplying the regional climate models.

## Funding sources

This work was supported by the Swiss Competence Center for Energy Research-Supply of Electricity (http://www.sccer-soe.ch).

## Appendix A. Supplementary material

Supplementary data to this article can be found online at https://doi.org/10.1016/j.jhydrol.2019.02.010.

## References

Addor, N., et al., 2014. Robust changes and sources of uncertainty in the projected hydrological regimes of Swiss catchments. Water Resour. Res. 50 (10), 7541–7562. https://doi.org/10.1002/2014wr015549.

Alexander, L.V., Arblaster, J.M., 2009. Assessing trends in observed and modelled climate extremes over Australia in relation to future projections. Int. J. Climatol. 29 (3), 417–435. https://doi.org/10.1002/joc.1730.

Anandhi, A., et al., 2011. Examination of change factor methodologies for climate change impact assessment. Water Resour. Res. 47 (3). https://doi.org/10.1029/2010WR009104.

Bartók, B., et al., 2017. Projected changes in surface solar radiation in CMIP5 global climate models and in EURO-CORDEX regional climate models for Europe. Clim. Dyn. 49 (7), 2665–2683. https://doi.org/10.1007/s00382-016-3471-2.

Blenkinsop, S., et al., 2013. Downscaling transient climate change with a stochastic weather generator for the Geer catchment, Belgium. Clim. Res. 57 (2), 95–109. https://doi.org/10.3354/cr01170.

Bordoy, R., Burlando, P., 2014. Stochastic downscaling of climate model precipitation outputs in orographically complex regions: 2. Downscaling methodology. Water Resour. Res. 50 (1), 562–579. https://doi.org/10.1002/wrcr.20443.

Burlando, M., Carassale, L., Georgieva, E., Ratto, C.F., Solari, G., 2007. A simple and efficient procedure for the numerical simulation of wind fields in complex terrain. Bound.-Layer Meteorol. 125 (3), 417–439. https://doi.org/10.1007/s10546-007-9196-3.

Burlando, P., Rosso, R., 1991. Extreme storm rainfall and climatic change. Atmos. Res. 27 (1), 169–189. https://doi.org/10.1016/0169-8095(91)90017-Q.

Burlando, P., Rosso, R., 2002. Effects of transient climate change on basin hydrology. 1. Precipitation scenarios for the Arno River, central Italy. Hydrol. Process. 16 (6), 1151–1175. https://doi.org/10.1002/hyp.1055.

Burton, A., Fowler, H.J., Blenkinsop, S., Kilsby, C.G., 2010. Downscaling transient climate change using a Neyman-Scott Rectangular Pulses stochastic rainfall model. J. Hydrol. 381 (1–2), 18–32. https://doi.org/10.1016/j.jhydrol.2009.10.031.

Camici, S., Brocca, L., Melone, F., Moramarco, T., 2014. Impact of climate change on flood frequency using different climate models and downscaling approaches. J. Hydrol. Eng. 19 (8), 04014002. https://doi.org/10.1061/(ASCE)HE.1943-5584.0000959.

Camici, S., Brocca, L., Moramarco, T., 2017. Accuracy versus variability of climate projections for flood assessment in central Italy. Clim. Change 141 (2), 273–286. https://doi.org/10.1007/s10584-016-1876-x.

Caracciolo, D., Noto, L.V., Istanbulluoglu, E., Fatichi, S., Zhou, X., 2014. Climate change and Ecotone boundaries: Insights from a cellular automata ecohydrology model in a Mediterranean catchment with topography controlled vegetation patterns. Adv. Water Resour. 73, 159–175. https://doi.org/10.1016/j.advwatres.2014.08.001.

Chen, Y., Hall, A., Liou, K.N., 2006. Application of three-dimensional solar radiative transfer to mountains. J. Geophys. Res.: Atmos. 111 (D21). https://doi.org/10.1029/2006JD007163. n/a-n/a.

Christensen, N.S., Wood, A.W., Voisin, N., Lettenmaier, D.P., Palmer, R.N., 2004. The effects of climate change on the hydrology and water resources of the Colorado River basin. Clim. Change 62 (1–3), 337–363. https://doi.org/10.1023/B:CLIM.0000013684.13621.1f.

Condon, L.E., Maxwell, R.M., 2015. Evaluating the relationship between topography and groundwater using outputs from a continental-scale integrated hydrology model. Water Resour. Res. 51 (8), 6602–6621. https://doi.org/10.1002/2014WR016774.

Curtis, D.C., Eagleson, P.S., 1982. Constrained stochastic climate simulation. Ralph M. Parsons laboratory, hydrology and water resource systems, massachusetts institute of technology. Department Civil Eng.

Deser, C., Knutti, R., Solomon, S., Phillips, A.S., 2012b. Communication of the role of natural variability in future North American climate. Nat. Clim. Change 2, 775. https://doi.org/10.1038/nclimate1562.

Deser, C., Phillips, A., Bourdette, V., Teng, H., 2012a. Uncertainty in climate change projections: the role of internal variability. Clim. Dyn. 38 (3), 527–546. https://doi.org/10.1007/s00382-010-0977-x.

Deser, C., Phillips, A.S., Alexander, M.A., Smoliak, B.V., 2014. Projecting North American climate over the next 50 years: uncertainty due to internal variability. J. Clim. 27 (6), 2271–2296. https://doi.org/10.1175/jcli-d-13-00451.1.

Dubayah, R., Loechel, S., 1997. Modeling topographic solar radiation using GOES data. J. Appl. Meteorol. 36 (2), 141–154.

Eagleson, P.S., 2005. Ecohydrology: Darwinian expression of vegetation form and function. Cambridge University Press.

Efron, B., 1979. 1977 Bootstrap methods - another look at the jackknife. Ann. Stat. 7 (1), 1–26. https://doi.org/10.1214/aos/1176344552.

Ehret, U., Zehe, E., Wulfmeyer, V., Warrach-Sagi, K., Liebert, J., 2012. HESS Opinions "Should we apply bias correction to global and regional climate model data?". Hydrol. Earth Syst. Sci. 16 (9), 3391–3404. https://doi.org/10.5194/hess-16-3391-2012.

Endrizzi, S., Gruber, S., Dall'Amico, M., Rigon, R., 2014. GEOtop 2.0: simulating the

combined energy and water balance at and below the land surface accounting for soil freezing, snow cover and terrain effects. Geosci. Model Dev. 7 (6), 2831–2857. https://doi.org/10.5194/gmd-7-2831-2014.
Fatichi, S., et al., 2016a. Uncertainty partition challenges the predictability of vital details of climate change. Earths Future 4 (5), 240–251. https://doi.org/10.1002/2015ef000336.
Fatichi, S., et al., 2016b. An overview of current applications, challenges, and future trends in distributed process-based models in hydrology. J. Hydrol. 537, 45–60. https://doi.org/10.1016/j.jhydrol.2016.03.026.
Fatichi, S., Ivanov, V.Y., Caporali, E., 2011. Simulation of future climate scenarios with a weather generator. Adv. Water Resour. 34 (4), 448–467. https://doi.org/10.1016/j.advwatres.2010.12.013.
Fatichi, S., Ivanov, V.Y., Caporali, E., 2013. Assessment of a stochastic downscaling methodology in generating an ensemble of hourly future climate time series. Clim. Dyn. 40 (7), 1841–1861. https://doi.org/10.1007/s00382-012-1627-2.
Fatichi, S., Rimkus, S., Burlando, P., Bordoy, R., Molnar, P., 2015. High-resolution distributed analysis of climate and anthropogenic changes on the hydrology of an Alpine catchment. J. Hydrol. 525, 362–382. https://doi.org/10.1016/j.jhydrol.2015.03.036.
Fealy, R., Sweeney, J., 2007. Statistical downscaling of precipitation for a selection of sites in Ireland employing a generalised linear modelling approach. Int. J. Climatol. 27 (15), 2083–2094. https://doi.org/10.1002/joc.1506.
Fowler, H.J., Kilsby, C.G., O'Connell, P.E., 2000. A stochastic rainfall model for the assessment of regional water resource systems under changed climatic conditions. Hydrol. Earth Syst. Sci. 4 (2), 263–282. https://doi.org/10.5194/hess-4-263-2000.
Fowler, H.J., Kilsby, C.G., O'Connell, P.E., Burton, A., 2005. A weather-type conditioned multi-site stochastic rainfall model for the generation of scenarios of climatic variability and change. J. Hydrol. 308 (1–4), 50–66. https://doi.org/10.1016/j.jhydrol.2004.10.021.
Fowler, H.J., Blenkinsop, S., Tebaldi, C., 2007. Linking climate change modelling to impacts studies: recent advances in downscaling techniques for hydrological modelling. Int. J. Climatol. 27 (12), 1547–1578. https://doi.org/10.1002/joc.1556.
Ghil, M., 2002. Natural climate variability. In: MacCracken, M.C., Perry, J.S. (Eds.), Encyclopedia of Global Environmental Change. John Wiley and Sons, Chichester.
Giorgi, F., 1990. Simulation of regional climate using a limited area model nested in a general-circulation model. J. Clim. 3 (9), 941–963.
Giorgi, F, 1995. Perspectives for regional earth system modeling. Global Planet. Change 10 (1-4), 23–42. https://doi.org/10.1016/0921-8181(94)00018-9.
Giorgi, F., Jones, C., Asrar, G.R., 2009. Addressing climate information needs at the regional level: the CORDEX framework. World Meteorological Organization (WMO) Bulletin 58 (3), 175.
Giorgi, F., Mearns, L.O., 1991. Approaches to the simulation of regional climate change - a review. Rev. Geophys. 29 (2), 191–216. https://doi.org/10.1029/90rg02636.
Giuntoli, I., Villarini, G., Prudhomme, C., Hannah, D.M., 2018. Uncertainties in projected runoff over the conterminous United States. Clim. Change 150 (3), 149–162. https://doi.org/10.1007/s10584-018-2280-5.
Glenis, V., Pinamonti, V., Hall, J.W., Kilsby, C.G., 2015. A transient stochastic weather generator incorporating climate model uncertainty. Adv. Water Resour. 85, 14–26. https://doi.org/10.1016/j.advwatres.2015.08.002.
Gneiting, T., Kleiber, W., Schlather, M., 2010. Matern cross-covariance functions for multivariate random fields. J. Am. Stat. Assoc. 105 (491), 1167–1177. https://doi.org/10.1198/jasa.2010.tm09420.
Gutmann, E., Barstad, I., Clark, M., Arnold, J., Rasmussen, R., 2016. The Intermediate Complexity Atmospheric Research Model (ICAR). J. Hydrometeorol. 17 (3), 957–973. https://doi.org/10.1175/jhm-d-15-0155.1.
Hawkins, E., Sutton, R., 2009. The potential to narrow uncertainty in regional climate predictions. Bull. Am. Meteorol. Soc. 90 (8), 1095-+. https://doi.org/10.1175/2009bams2607.1.
Hawkins, E., Sutton, R., 2011. The potential to narrow uncertainty in projections of regional precipitation change. Clim. Dyn. 37 (1–2), 407–418. https://doi.org/10.1007/s00382-010-0810-6.
Heinrich, G., Gobiet, A., 2012. The future of dry and wet spells in Europe: a comprehensive study based on the ENSEMBLES regional climate models. Int. J. Climatol. 32 (13), 1951–1970. https://doi.org/10.1002/joc.2421.
Hewitson, B.C., Crane, R.G., 1996. Climate downscaling: Techniques and application. Clim. Res. 7 (2), 85–95. https://doi.org/10.3354/cr007085.
Hingray, B., Said, M., 2014. Partitioning internal variability and model uncertainty components in a multimember multimodel ensemble of climate projections. J. Clim. 27 (17), 6779–6798. https://doi.org/10.1175/jcli-d-13-00629.1.
Hutchinson, M.F., 1995. Stochastic space-time weather models from ground-based data. Agric. For. Meteorol. 73 (3–4), 237–264. https://doi.org/10.1016/0168-1923(94)05077-j.
IPCC, 2018. Summary for Policymakers. In: Masson-Delmotte, V., Zhai, P., Pörtner, H.-O., Roberts, D., Skea, J., Shukla, P.R., Pirani, A., Moufouma-Okia, Péan, C., Pidcock, R., Connors, S., Matthews, J.B.R., Chen, Y., Zhou, X., Gomis, M.I., Lonnoy, E., Maycock, Tignor, M., Waterfield, T., (Eds.), *Global Warming of 1.5°C. An IPCC Special Report on the impacts of global warming of 1.5°C above pre-industrial levels and related global greenhouse gas emission pathways, in the context of strengthening the global response to the threat of climate change, sustainable development, and efforts to eradicate poverty*. World Meteorological Organization, Geneva, Switzerland, pp. 32.
Ivanov, V.Y., Vivoni, E.R., Bras, R.L., Entekhabi, D., 2004. Preserving high-resolution surface and rainfall data in operational-scale basin hydrology: a fully-distributed physically-based approach. J. Hydrol. 298 (1), 80–111. https://doi.org/10.1016/j.jhydrol.2004.03.041.
Ivanov, V.Y., Bras, R.L., Curtis, D.C., 2007. A weather generator for hydrological, ecological, and agricultural applications. Water Resour. Res. 43 (10). https://doi.org/10.1029/2006wr005364.
Themeßl, M.J., Gobiet, A., Leuprecht, A., 2011. Empirical-statisticaldownscaling and error correction of daily precipitation from regional climate models. Int. J. Climatol. 31 (10), 1530–1544. https://doi.org/10.1002/joc.2168.
Johnson, N.L., 1949. Systems of frequency curves generated by methods of translation. Biometrika 36 (1–2), 149–176. https://doi.org/10.2307/2332539.
Juszak, I., Pellicciotti, F., 2013. A comparison of parameterizations of incoming longwave radiation over melting glaciers: Model robustness and seasonal variability. J. Geophys. Res.-Atmos. 118 (8), 3066–3084. https://doi.org/10.1002/jgrd.50277.
Katz, R.W., 1996. Use of conditional stochastic models to generate climate change scenarios. Clim. Change 32 (3), 237–255. https://doi.org/10.1007/bf00142464.
Katz, R.W., Parlange, M.B., 1998. Overdispersion phenomenon in stochastic modeling of precipitation. J. Clim. 11 (4), 591–601.
Keller, D.E., et al., 2015. Implementation and validation of a Wilks-type multi-site daily precipitation generator over a typical Alpine river catchment. Hydrol. Earth Syst. Sci. 19 (5), 2163–2177. https://doi.org/10.5194/hess-19-2163-2015.
Kerr, R.A., 2011. Predicting climate change vital details of global warming are eluding forecasters. Science 334 (6053), 173–174. https://doi.org/10.1126/science.334.6053.173.
Kilsby, C.G., et al., 2007. A daily weather generator for use in climate change studies. Environ. Modell. Software 22 (12), 1705–1719. https://doi.org/10.1016/j.envsoft.2007.02.005.
Kim, J., Ivanov, V.Y., Fatichi, S., 2016. Climate change and uncertainty assessment over a hydroclimatic transect of Michigan. Stoch. Env. Res. Risk Assess. 30 (3), 923–944. https://doi.org/10.1007/s00477-015-1097-2.
Knutti, R., Masson, D., Gettelman, A., 2013. Climate model genealogy: Generation CMIP5 and how we got there. Geophys. Res. Lett. 40 (6), 1194–1199. https://doi.org/10.1002/grl.50256.
Kotlarski, S., et al., 2014. Regional climate modeling on European scales: a joint standard evaluation of the EURO-CORDEX RCM ensemble. Geosci. Model Dev. 7 (4), 1297–1333. https://doi.org/10.5194/gmd-7-1297-2014.
Lang, A., Potthoff, J., 2011. Fast simulation of Gaussian random fields. Monte Carlo Methods Appl. 17 (3), 195–214. https://doi.org/10.1515/mcma.2011.009.
Leutwyler, D., Fuhrer, O., Lapillonne, X., Luthi, D., Schar, C., 2016. Towards European-scale convection-resolving climate simulations with GPUs: a study with COSMO 4.19. Geosci. Model Develop. 9 (9), 3393–3412. https://doi.org/10.5194/gmd-9-3393-2016.
Marani, M., 2005. Non-power-law-scale properties of rainfall in space and time. Water Resour. Res. 41 (8). https://doi.org/10.1029/2004WR003822.
Maraun, D., et al., 2010. Precipitation downscaling under climate change: Recent developments to bridge the gap between dynamical models and the end user. Rev. Geophys. 48 (3). https://doi.org/10.1029/2009RG000314.
Marra, F., Morin, E., Peleg, N., Mei, Y.W., Anagnostou, E.N., 2017. Intensity-duration-frequency curves from remote sensing rainfall estimates: comparing satellite and weather radar over the eastern Mediterranean. Hydrol. Earth Syst. Sci. 21 (5), 2389–2404. https://doi.org/10.5194/hess-21-2389-2017.
Meinshausen, M., et al., 2011. The RCP greenhouse gas concentrations and their extensions from 1765 to 2300. Clim. Change 109 (1), 213. https://doi.org/10.1007/s10584-011-0156-z.
Murphy, J., 1999. An evaluation of statistical and dynamical techniques for downscaling local climate. J. Clim. 12 (8), 2256–2284.
Olonscheck, D., Notz, D., 2017. Consistently estimating internal climate variability from climate model simulations. J. Clim. 30 (23), 9555–9573. https://doi.org/10.1175/jcli-d-16-0428.1.
Park, J.Y., Kim, S.J., 2014. Potential impacts of climate change on the reliability of water and hydropower supply from a multipurpose dam in South Korea. J. Am. Water Resour. Assoc. 50 (5), 1273–1288. https://doi.org/10.1111/jawr.12190.
Park, J., Onof, C., Kim, D., 2018. A hybrid stochastic rainfall model that reproduces rainfall characteristics at hourly through yearly time scale. Hydrol. Earth Syst. Sci. Discuss. 2018, 1–31. https://doi.org/10.5194/hess-2018-267.
Paschalis, A., Molnar, P., Fatichi, S., Burlando, P., 2013. A stochastic model for high-resolution space-time precipitation simulation. Water Resour. Res. 49 (12), 8400–8417. https://doi.org/10.1002/2013wr014437.
Paschalis, A., Fatichi, S., Molnar, P., Rimkus, S., Burlando, P., 2014. On the effects of small scale space-time variability of rainfall on basin flood response. J. Hydrol. 514, 313–327. https://doi.org/10.1016/j.jhydrol.2014.04.014.
Peleg, N., et al., 2018. Spatial variability of extreme rainfall at radar subpixel scale. J. Hydrol. 556, 922–933. https://doi.org/10.1016/j.jhydrol.2016.05.033.
Peleg, N., Bartov, M., Morin, E., 2015a. CMIP5-predicted climate shifts over the East Mediterranean: implications for the transition region between Mediterranean and semi-arid climates. Int. J. Climatol. 35 (8), 2144–2153. https://doi.org/10.1002/joc.4114.
Peleg, N., Shamir, E., Georgakakos, K.P., Morin, E., 2015b. A framework for assessing hydrological regime sensitivity to climate change in a convective rainfall environment: a case study of two medium-sized eastern Mediterranean catchments. Israel. Hydrol. Earth Syst. Sci. 19 (1), 567–581. https://doi.org/10.5194/hess-19-567-2015.
Peleg, N., Blumensaat, F., Molnar, P., Fatichi, S., Burlando, P., 2017a. Partitioning the impacts of spatial and climatological rainfall variability in urban drainage modeling. Hydrol. Earth Syst. Sci. 21 (3), 1559–1572. https://doi.org/10.5194/hess-21-1559-2017.
Peleg, N., Fatichi, S., Paschalis, A., Molnar, P., Burlando, P., 2017b. An advanced stochastic weather generator for simulating 2-D high-resolution climate variables. J. Adv. Model. Earth Syst. 9 (3), 1595–1627. https://doi.org/10.1002/2016ms000854.
Peleg, N., Morin, E., 2014. Stochastic convective rain-field simulation using a high-resolution synoptically conditioned weather generator (HiReS-WG). Water Resour. Res. 50 (3), 2124–2139. https://doi.org/10.1002/2013wr014836.
Perra, E., et al., 2018. Multimodel assessment of climate change-induced hydrologic

impacts for a Mediterranean catchment. Hydrol. Earth Syst. Sci. 22 (7), 4125–4143. https://doi.org/10.5194/hess-22-4125-2018.
Prein, A.F., et al., 2015. A review on regional convection-permitting climate modeling: Demonstrations, prospects, and challenges. Rev. Geophys. 53 (2), 323–361. https://doi.org/10.1002/2014rg000475.
Prein, A.F., et al., 2016. Precipitation in the EURO-CORDEX 0.11∘ and 0.44∘ simulations: high resolution, high benefits? Clim. Dyn. 46 (1), 383–412. https://doi.org/10.1007/s00382-015-2589-y.
Rienecker, M.M., et al., 2011. MERRA: NASA's Modern-Era retrospective analysis for research and applications. J. Clim. 24 (14), 3624–3648. https://doi.org/10.1175/jcli-d-11-00015.1.
Schneider, T., Neumaier, A., 2001. Algorithm 808: ARfit - A matlab package for the estimation of parameters and eigenmodes of multivariate autoregressive models. Acm Trans. Math. Softw. 27 (1), 58–65. https://doi.org/10.1145/382043.382316.
Schulla, J., Jasper, K., 2007. Model description Wasim-ETH. Institute for Atmospheric and Climate Science, Swiss Federal Institute of Technology, Zurich.
Semenov, M.A., Barrow, E.M., 1997. Use of a stochastic weather generator in the development of climate change scenarios. Clim. Change 35 (4), 397–414. https://doi.org/10.1023/a:1005342632279.
Sexton, D.M.H., Harris, G.R., 2015. The importance of including variability in climate change projections used for adaptation. Nat. Clim. Change 5, 931. https://doi.org/10.1038/nclimate2705.
Singer, M.B., Michaelides, K., 2017. Deciphering the expression of climate change within the Lower Colorado River basin by stochastic simulation of convective rainfall. Environ. Res. Lett. 12 (10), 104011. https://doi.org/10.1088/1748-9326/aa8e50.
Singer, M.B., Michaelides, K., Hobley, D.E.J., 2018. STORM: A simple, flexible, and parsimonious stochastic rainfall generator for simulating climate and climate change. Geosci. Model Dev. Discuss. 2018, 1–25. https://doi.org/10.5194/gmd-2018-86.
Slingo, J., Palmer, T., 2011. Uncertainty in weather and climate prediction. Philos. Trans. Royal Soc. A: Math., Phys. Eng. Sci. 369 (1956), 4751–4767. https://doi.org/10.1098/rsta.2011.0161.
Svoboda, V., Hanel, M., Máca, P., Kyselý, J., 2016. Projected changes of rainfall event characteristics for the Czech Republic. J. Hydrol. Hydromech. 415. https://doi.org/10.1515/johh-2016-0036.
Tebaldi, C., Smith, R.L., Nychka, D., Mearns, L.O., 2005. Quantifying uncertainty in projections of regional climate change: a Bayesian approach to the analysis of multimodel ensembles. J. Clim. 18 (10), 1524–1540. https://doi.org/10.1175/JCLI3363.1.
Teutschbein, C., Seibert, J., 2012. Bias correction of regional climate model simulations for hydrological climate-change impact studies: Review and evaluation of different methods. J. Hydrol. 456, 12–29. https://doi.org/10.1016/j.jhydrol.2012.05.052.
Teutschbein, C., Wetterhall, F., Seibert, J., 2011. Evaluation of different downscaling techniques for hydrological climate-change impact studies at the catchment scale. Clim. Dyn. 37 (9–10), 2087–2105. https://doi.org/10.1007/s00382-010-0979-8.
van Vuuren, D.P., et al., 2011. The representative concentration pathways: an overview. Clim. Change 109 (1), 5. https://doi.org/10.1007/s10584-011-0148-z.
Wasko, C., Sharma, A., 2017. Continuous rainfall generation for a warmer climate using observed temperature sensitivities. J. Hydrol. 544, 575–590. https://doi.org/10.1016/j.jhydrol.2016.12.002.
Wheater, H.S., et al., 2005. Spatial-temporal rainfall modelling for flood risk estimation. Stoch. Env. Res. Risk Assess. 19 (6), 403–416. https://doi.org/10.1007/s00477-005-0011-8.
Wilby, R.L., Wigley, T.M.L., 1997. Downscaling general circulation model output: a review of methods and limitations. Prog. Phys. Geogr. 21 (4), 530–548. https://doi.org/10.1177/030913339702100403.
Wilks, D.S., Wilby, R.L., 1999. The weather generation game: a review of stochastic weather models. Prog. Phys. Geogr. 23 (3), 329–357. https://doi.org/10.1177/030913339902300302.
Wood, A.W., Leung, L.R., Sridhar, V., Lettenmaier, D.P., 2004. Hydrologic implications of dynamical and statistical approaches to downscaling climate model outputs. Clim. Change 62 (1–3), 189–216. https://doi.org/10.1023/B:CLIM.0000013685.99609.9e.
Xu, C.Y., 1999. Climate change and hydrologic models: A review of existing gaps and recent research developments. Water Resour. Manage. 13 (5), 369–382. https://doi.org/10.1023/a:1008190900459.
Xu, D., Ivanov, V.Y., Kim, J., Fatichi, S., 2018. On the use of observations in assessment of multi-model climate ensemble. Stoch. Env. Res. Risk Assess. https://doi.org/10.1007/s00477-018-1621-2.
Xu, C.Y., Widen, E., Halldin, S., 2005. Modelling hydrological consequences of climate change - Progress and challenges. Adv. Atmos. Sci. 22 (6), 789–797. https://doi.org/10.1007/bf02918679.